Journal of Organometallic Chemistry 706-707 (2012) 52–65

Contents lists available at SciVerse ScienceDirect

Journal of Organometallic Chemistry

journal homepage: www.elsevier.com/locate/jorganchem

Fundamental study of (ferrocenylethynyl)phosphines: Correlation of steric and electronic effects in *C,C* cross-coupling reactions

Bianca Milde, Dieter Schaarschmidt, Petra Ecorchard, Heinrich Lang*

Chemnitz University of Technology, Faculty of Science, Institute of Chemistry, Department of Inorganic Chemistry, Straße der Nationen 62, 09111 Chemnitz, Germany

ARTICLE INFO

Article history:
Received 22 September 2011
Received in revised form
16 January 2012
Accepted 23 January 2012

Keywords:
(Ferrocenylethynyl)phosphine
Palladium
Seleno phosphine
(Spectro-) electrochemistry
Tolman cone angle
C,C cross-coupling

ABSTRACT

Complexes $[Pd(Cl)(\mu\text{-}Cl)(P(C{\equiv}CFc)R_2)]_2$ (Fc = $(\eta^5\text{-}C_5H_4)(\eta^5\text{-}C_5H_5)$; **6e**, *R* = ^{t}Bu; **6f**, *R* = $^c C_6H_{11}$) and $[PdCl_2(P(C{\equiv}CFc)R_2)_2]$ (**7a**, *R* = C_6H_5; **7b**, *R* = 2-MeC_6H_4; **7c**, *R* = 2,4,6-$Me_3C_6H_2$; **7d**, *R* = $^c C_4H_3O$; **7e**, *R* = ^{t}Bu; **7f**, *R* = $^c C_6H_{11}$) are accessible by the reaction of $P(C{\equiv}CFc)R_2$ (**3a**–**f**) with either $[PdCl_2(cod)]$ (**5**) (cod = cyclo-1,5-octadiene) or $[PdCl_2(SEt_2)_2]$ (**8**). The spectroscopic, mass-spectrometric and cyclovoltammetric data of **6** and **7** were investigated and the structures of four complexes (**6e**, **6f**, **7b**, **7c**) in the solid state determined. Complexes **7a**–**f** are mononuclear with palladium in a square-planar environment and show a *cis*- (**7b**) or *trans*-configuration (**7c**) with linear FcC≡CP moieties in the solid state. In contrast, **6e** and **6f** are forming dimers with a planar $Pd_2P_2Cl_2(\mu\text{-}Cl)_2$ core with the ferrocenylethynyl ligands positioned above and below this plane. Electrochemical studies of phosphines **3a**–**3f** and the appropriate seleno phosphines **4a**–**4f** show after oxidation follow-up reactions, while a reversible behavior is found for the corresponding palladium complexes **6** and **7**. UV–Vis/NIR and IR spectro–electrochemical measurements of **7f** indicate moderate electronic interactions between the ferrocenyl units. All complexes are catalytically active in Heck (reaction of iodo benzene with *tert*-butyl acrylate) and Suzuki (2-bromo toluene or 4′-chloro acetophenone with phenyl boronic acid) *C,C* cross-couplings. The influence of the electronic ($^1J(^{31}P{-}^{77}Se)$) and the steric (Tolman cone angle) properties of the phosphine ligands on the activity of the respective palladium catalysts will be discussed.

1. Introduction

Recently, alkynyl phosphines of general type $P(C{\equiv}CR')_nR_{3-n}$ ($n = 1, 2, 3$; $R, R' =$ organic or organometallic single-bonded group; $R = R'$; $R \neq R'$) have come into focus because they are of interest due to their versatile reaction chemistry toward different organometallic and metal–organic compounds leading into the area of, for example, clusters [1], coordination polymers [2], polynuclear complexes [2b,c,3], or metallacycles [4]. The properties of alkynyl phosphines are unique including their structure, chemical behavior, reactivity, and catalytic activity. The reaction chemistry of these molecules is driven either by the fact that they act as *P* and/or C≡C donors toward metal species or by the cleavage of the $P{-}C_{alkynyl}$ bond induced by thermolysis, photolysis or chemical activation resulting in the formation of phosphido and acetylide fragments, respectively [2a,4b,5]. In addition, (ferrocenylethynyl)phosphines have gained attraction in supra- and macro-molecular chemistry allowing the development of new materials with peculiar physical and chemical properties [5b,6]. Just as the alkynyl phosphines, (ferrocenylethynyl)phosphines found use as ligands in homogeneous *C,C* cross-coupling reactions (Heck and Suzuki) [2c,7], and as redox-active compounds to study multinuclear redox processes [5c,6,8]. Palladium-promoted Suzuki and Heck carbon–carbon cross-couplings represent one of the most effective transformations in organometallic and organic synthesis. The Heck reaction allows to convert (un)saturated halides or triflates into substituted alkenes in a very efficient, convenient and inexpensive way in the presence of a base and a palladium source [9]. In this respect, most active catalysts are bulky, electron-rich phosphine- [10], NHC- [11], and biphenyl phosphine-based palladium complexes [12], as well as phosphapalladacycles [12b,13]. The Suzuki reaction is the conversion of aryl- or vinyl-boronic acids with an aryl- or vinyl-halide to polyolefins, styrenes, and substituted biphenyls, and has been extended to incorporate alkyl bromides in the presence of palladium [9].

In this work we present the synthesis of a series of (ferrocenylethynyl)phosphines and their reaction behavior toward selenium and palladium dichloride. The utilization of the appropriate phosphine palladium dichlorides in Heck and Suzuki *C,C* couplings is reported as well.

* Corresponding author. Tel.: +49 0 371 531 21210; fax: +49 0 371 531 21219.
E-mail address: heinrich.lang@chemie.tu-chemnitz.de (H. Lang).

0022-328X/$ – see front matter © 2012 Elsevier B.V. All rights reserved.
doi:10.1016/j.jorganchem.2012.01.017

2. Results and discussion

2.1. Synthesis, reaction chemistry and characterization

(Ferrocenylethynyl)phosphines P(C≡CFc)R_2 (Fc = (η^5-C_5H_4)(η^5-C_5H_5); **3a**, $R = C_6H_5$ [6b]; **3b**, R = 2-MeC_6H_4; **3c**, R = 2,4,6-$Me_3C_6H_2$; **3d**, $R = {}^cC_4H_3O$; **3e**, $R = {}^t$Bu; **3f**, $R = {}^cC_6H_{11}$) were synthesized by reacting FcC≡CH (**1**) with one equivalent of ^{n}butyllithium and subsequent treatment with ClPR_2 (**2a**–**f**) (Reaction 1).

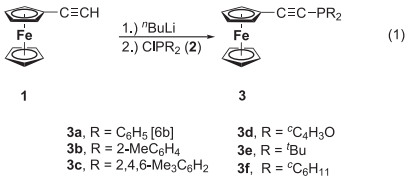

To obtain 1st information on the Lewis-basicity of phosphines **3a**–**f** we prepared the respective seleno phosphines (Se)P(C≡CFc)R_2 (**4a**–**f**) by treatment of **3a**–**f** with elemental selenium in toluene at 100 °C (Experimental Section). Seleno phosphines **4a**–**f** could be isolated in virtually quantitative yield as yellow to orange solids.

Addition of [PdCl_2(cod)] (**5**) (cod = cyclo-1,5-octadiene) to dichloromethane solutions containing **3a**–**f** in a molar ratio of 1:2 gave complexes [Pd(Cl)(μ-Cl)(P(C≡CFc)R_2)]$_2$ (**6e**, $R = {}^t$Bu; **6f**, $R = {}^cC_6H_{11}$) and *cis*/*trans*-[PdCl_2(P(C≡CFc)R_2)$_2$] (**7a**, $R = C_6H_5$; **7b**, R = 2-MeC_6H_4; **7c**, R = 2,4,6-$Me_3C_6H_2$; **7d**, $R = {}^cC_4H_3O$), respectively (Scheme 1). While the formation of **7a**–**d** is expected, the building of **6e** and **6f** surprises at first. The latter complexes are also generated, when repeating the reactions in a 1:1 M ratio. From these reactions it is obvious that the alkyl groups R at phosphorus favor the formation of a palladium dimer with a planar Pd$_2$(μ-Cl)$_2$ four-membered cycle, while aryl substituents solely gave mononuclear **7a**–**d** as it could be proven by single X-ray structure determination (see below). For bulky substituents at phosphorus this reaction behavior is a known phenomenon [14]. It can be explained by the different solubility of the palladium sources and the formed complexes in dichloromethane [14a] as well as the size of their coordinated ligands (*e.g.*, NCMe, cod) [14f]. Another straightforward synthesis methodology to prepare **7a**–**f** is given by treatment of **3a**–**f** with the palladium source [PdCl_2(SEt$_2$)$_2$] (**8**) (Scheme 1). However, by this reaction exclusively **7a**–**f** are formed.

Seleno phosphines **4a**–**f** as well as complexes **6e**, **f** and **7a**–**f** are stable in air and moisture both in the solid state and in solution, whereas **3a**–**f** slowly oxidize in solution. All compounds have been identified by elemental analysis as well as by IR and NMR (^{1}H, ^{13}C{^{1}H}, ^{31}P{^{1}H}) spectroscopy. High resolution-ESI-TOF mass-spectrometry and single crystal X-ray structure analysis (**6e**, **6f**, **7b** and **7c**) were additionally carried out. The electrochemical behavior of the newly prepared compounds (cyclic voltammetry (CV) (**3**, **4**, **6** and **7**), square wave voltammetry (SWV) (**6**, **7**), linear sweep voltammetry (LSV) (**7**), UV–Vis/NIR spectroscopy (280–3000 nm) and *in situ* IR spectroscopy (**7f**)) is discussed as well.

Single crystals of **6e**, **6f**, *cis*-**7b**, and *trans*-**7c** suitable for X-ray diffraction studies could be obtained by diffusion of ^{n}hexane or diethyl ether into chloroform solutions containing the appropriate complexes at ambient temperature. The molecular structures of **6e** and **6f** in the solid state are shown in Fig. 1, the ones of *cis*-**7b** and *trans*-**7c** in Fig. 2. Important bond distances (Å), bond angles (°) and torsion angels (°) are summarized in Table 1. For crystal and structure refinement data see Experimental Section.

Complexes **6e** and **6f** crystallize in the triclinic space group $P\bar{1}$ as red needles. Both species are *iso*-structural possessing Pd$_2$P$_2$Cl$_2$(μ-Cl)$_2$ moieties featuring a crystallographically imposed inversion symmetry with the inversion center in the middle between the palladium atoms Pd1 and Pd1A (symmetry transformations used to generate equivalent atoms: −x+1, −y+1, −z+1) (Fig. 1). The (ferrocenylethynyl) groups are oppositely oriented with the ferrocenyl units above or below the slightly distorted square-planar Pd$_2$P$_2$Cl$_2$(μ-Cl)$_2$ core (**6e**: r. m. s. deviation 0.0120 Å, highest deviation from planarity observed for Pd1 with −0.0240 Å; **6f**: r.m.s. deviation 0.0049 Å, highest deviation from planarity observed for Pd1 with −0.0098 Å) with characteristic parameters for this type of compounds [14]. The Pd1–Cl2 and Pd1–Cl2A bond distances in **6e** and **6f** are asymmetric with the somewhat longer bonds situated opposite the more strongly *trans* influencing (ferrocenylethynyl)phosphine substituents (Table 1). Obviously, the palladium–chloride distances within the Pd$_2$(μ-Cl)$_2$ cycle (Pd1–Cl2: **6e**, 2.3176(6) Å; **6f**, 2.4479(6) Å) are longer as the terminal Pd1–Cl1 bonds (Pd1–Cl1: **6e**, 2.2755(6) Å; **6f**, 2.2729(6) Å) allegeable due to their different environment (Fig. 1, Table 1). The bond lengths and angles of the P–C units are comparable to those observed in similar species, *i.e.* [PdCl(μ-Cl)(PPh$_2^n$Pr)]$_2$ [14d] and [PdCl(μ-Cl)(P($^cC_4H_3O$)$_3$)]$_2$ [14b], respectively. The (ethynyl)phosphine units are essentially linear (Table 1) which is in contrast to other (ferrocenylethynyl) palladium complexes, *e.g.* [PdCl_2(P(C≡CFc)Ph$_2$)$_2$] in which a significant deviation from linearity was found (P–C≡C: 171, 157°) [6b]. The cyclopentadienyl ligands at the iron centers show an almost staggered conformation (**6e**: 4.6°, **6f**: −2.7°).

In crystals of **7b** the molecules are packed in the monoclinic space group $C2/c$, in **7c** the crystals are packed in the triclinic space group $P\bar{1}$. Complex **7b** exhibits a mirror plane through the palladium center Pd1, while **7c** possesses an inversion center at the central palladium atom Pd1 (Fig. 2). The crystal structure analysis

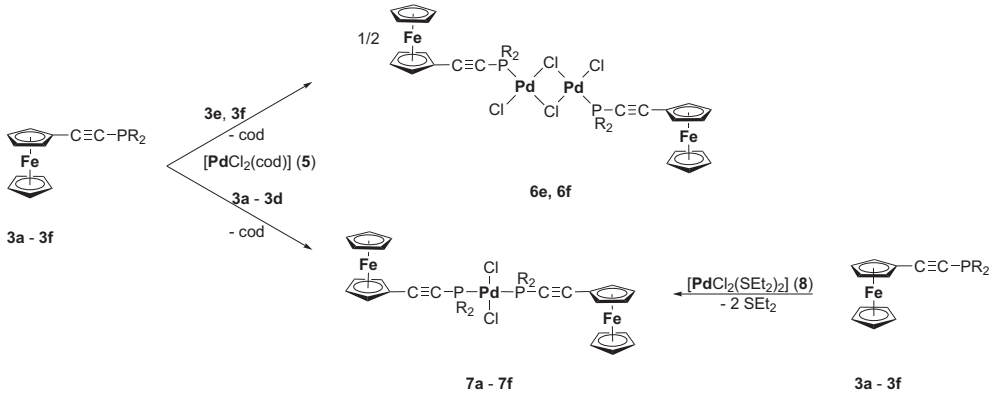

Scheme 1. Synthesis of **6e**, **6f** and **7a**–**7f** from **3**, **5**, and **8**.

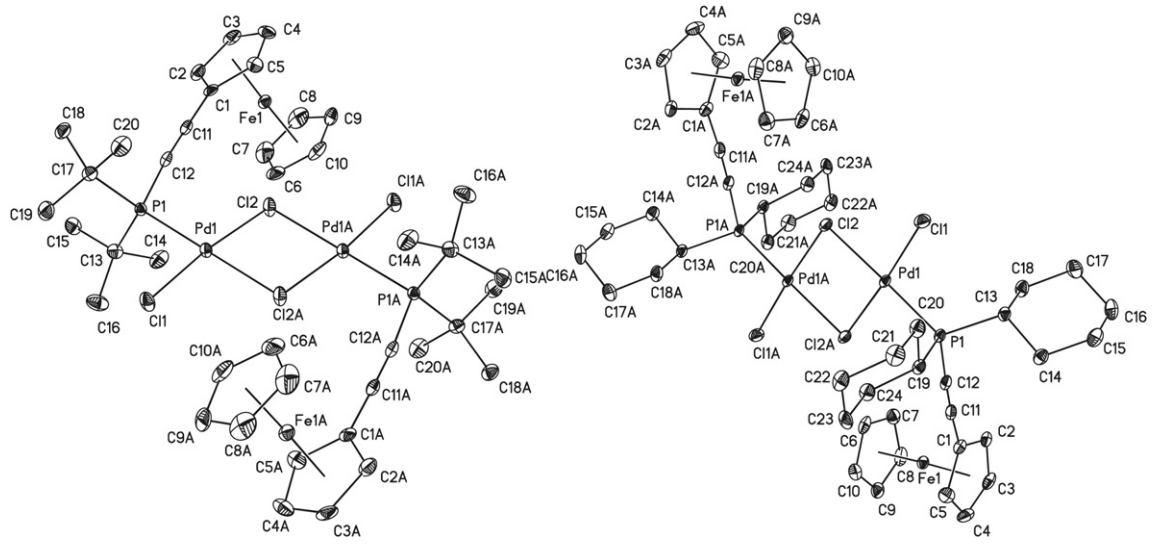

Fig. 1. ORTEP diagrams (50% probability level) of the molecular structures of **6e** (left) and **6f** (right) with the atom-numbering scheme. All hydrogen atoms and two $CHCl_3$ solvent molecules (**6f**) have been omitted for clarity. For selected bond distances (Å), angles (°) and torsion angels (○) see Table 1. (Symmetry generated atoms are indicated by the suffix A; symmetry code: −x+1, −y+1, −z+1.)

showed that **7b** is *cis*-configurated, whereas **7c** owns a *trans* arrangement in the solid state (Fig. 2). *cis*-configuration is generally observed for (alkynyl)phosphine palladium chloride complexes, although corresponding palladium iodide species are *trans* oriented [6b]. However, in solution only one isomer exists, most likely showing the thermodynamically more stable *trans*-configuration as indicated by IR and NMR studies (vide infra). For both species, the complex geometries around palladium are square-planar as expected for a d^8 transition metal ion (**7b**: r.m.s. deviation 0.0728 Å, highest deviation from planarity observed for P1 with −0.0914 Å). Typical for **7b** is that the P−C≡C−C_{Fc} ligands are not coplanar to the PdP_2Cl_2 core, similar to [*M*(P(C≡CFc)Ph_2)$_2Cl_2$] (*M* = Pd, Pt), with a P−C≡C angle of 175.1(4)° (Table 1) [5c,6b,8]. In **7c** a coplanar *s-trans*-like structure for the (ferrocenylethynyl)phosphines is found (Fig. 2). The *trans* orientation in **7c**, compared to *cis*-**7b**, is most probably attributed to the larger substituents at phosphorus, which also has an influence on the linearity of the (alkynyl)phosphine units. The P−C≡C and C≡C−C_{Fc} angles in **7c** deviate more from linearity then the ones in **7b** (Table 1). All other structural parameters are similar to other (ferrocenyl) [6b] and (phenylethynyl) [2c] phosphine palladium complexes.

The completeness of the reaction of **1** with ^{n}BuLi/**2** to give **3** (Reaction 1) can be confirmed by IR spectroscopy, since the C≡C and ≡C−H vibrations of the HC≡C unit in **1** [30] at 2102 and 3279 cm^{-1}, respectively, disappear during the course of the reaction and new absorptions between 2140 and 2155 cm^{-1} appear which can be assigned to the $\nu_{C\equiv C}$ frequencies of the (ferrocenylethynyl) phosphines **3a**–**f** (Experimental Section). Oxidation of **3a**–**f** with

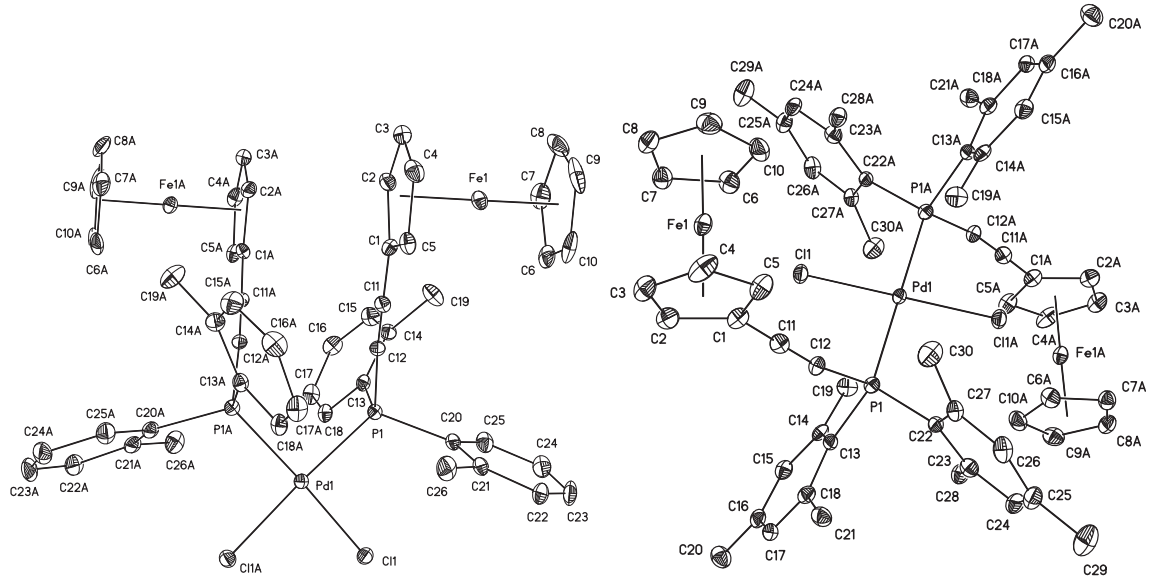

Fig. 2. ORTEP diagrams (30% (**7b**), 50% (**7c**) probability level) of the molecular structures of *cis*-**7b** (left) and *trans*-**7c** (right) with the atom-numbering scheme. All hydrogen atoms and two molecules of the solvent $CHCl_3$ (**7b**) have been omitted for clarity. For selected bond distances (Å), angles (°) and torsion angels (○) see Table 1. (Symmetry generated atoms are indicated by the suffix A; symmetry code: **7b**: −x, y, −z+1/2; **7c**: −x, −y, −z+2.)

Table 1
Selected bond lengths (Å), bond angles and torsion angles (°) for complexes **6e**, **6f**, **7b**, and **7c**.[a]

	6e	6f	7b	7c
Pd1–P1	2.2504(6)	2.2297(6)	2.2644(13)	2.3227(7)
Pd1–Cl1	2.2755(6)	2.2729(6)	2.3422(13)	2.3075(7)
Pd1–Cl2	2.3176(6)	2.4479(6)		
Pd1–Cl2A[c]	2.4081(5)	2.3341(6)		
P1–C12	1.748(2)	1.747(3)	1.732(5)	1.760(3)
P1–C13	1.874(2)	1.834(2)	1.814(5)	1.843(3)
P1–C17	1.882(2)			
P1–C19		1.839(2)		
P1–C20			1.829(5)	
P1–C22				1.833(3)
C1–C11	1.421(3)	1.426(4)	1.416(7)	1.434(4)
C11–C12	1.199(3)	1.203(4)	1.205(6)	1.201(4)
D1–Fe1[b]	1.6377(3)	1.6429(5)	1.6465(7)	1.6482(3)
D2–Fe2[b]	1.6468(3)	1.6503(5)	1.6513(7)	1.6548(3)
P1–Pd1–Cl1	91.89(2)	88.71(2)	88.09(4)	88.49(3)
P1–Pd1–Cl2	94.20(2)	178.81(2)		
P1–Pd1–Cl2A[c]	178.857(19)	94.37(2)		
P1–Pd1–P1A[c]			93.57(7)	180.0
P1–Pd1–Cl1A[c]			175.24(5)	91.51(2)
Pd1–Cl2–Pd1A[c]	94.992(19)	95.33(2)		
Cl1–Pd1–Cl2	173.64(2)	92.23(2)		
Cl1–Pd1–Cl1A[c]			90.61(6)	180.0
P1–C12–C11	175.46(19)	177.1(2)	175.1(4)	171.1(3)
C1–C11–C12	176.9(2)	176.2(3)	176.5(5)	173.6(3)
D1–Fe1–D2[b]	178.43(2)	176.86(4)	179.46(5)	178.94(3)
P1–C12–C11–C1	−66(5)	86(6)	129(7)	−106(3)
Pd1–P1–C12–C11	18(2)	75(5)	90(5)	−8.4(18)
Pd1–P1–C13–C14	−62.81(15)	−177.15(14)	161.0(3)	4.4(3)
Pd1–P1–C17–C18	156.65(13)			
Pd1–P1–C19–C20		−66.84(18)3		
Pd1–P1–C20–C21			−58.9(5)	
Pd1–P1–C22–C27				85.7(2)
Cl1–Pd1–P1–C12	170.44(7)	−155.11(9)	−148.92(18)	−48.97(10)
Cl1–P1–Pd1–C13	−77.47(8)	−36.74(9)	90.94(17)	64.74(11)
Cl1–P1–Pd1–C17	56.83(8)			
Cl1–P1–Pd1–C19		87.92(9)		
Cl1–Pd1–P1–C20			−32.4(2)	
Cl1–Pd1–P1–C22				−165.81(11)

[a] Standard uncertainties of the last significant digit(s) are shown in parenthesis.
[b] D1 denotes the centroid of C_5H_4 at Fe1; D2 denotes the centroid of C_5H_5 at Fe1.
[c] Symmetry generated atoms (for symmetry code see Figs. 1 and 2).

selenium in its elemental form to afford the seleno phosphines **4a**–**f** as well as the coordination of the phosphorus atoms of **3a**–**3f** to palladium(II) to produce the corresponding phosphine palladium complexes **6** and **7** resulted in a shift of the $\nu_{C\equiv C}$ bands to higher wavenumbers, which is typical for these reactions (Experimental Section) [6b]. Next to IR also $^{13}C\{^1H\}$ and $^{31}P\{^1H\}$ NMR spectroscopy allows to monitor the reaction progress owing to the C≡C units and the phosphorus atoms present in **1**, **3**, **4**, **6**, and **7** (Experimental Section). In this respect, most indicative is $^{31}P\{^1H\}$ NMR spectroscopy. It was found that upon coordination of the phosphorus atom to palladium a shift to lower field is observed, *i. e.* **3b**: −47.7 ppm, **7b**: −6.8 ppm (Experimental Section). Changing the phosphorus oxidation state of III in **3** to V in **4** also induces, as expected, a significant down-field shift (*i. e.*, **3b**: −47.7 ppm; **4b**: 0.9 ppm). In general, the donor capacity of phosphines PRR′*R*″ ($R = R' = R''$; $R \neq R' \neq R''$; *R*, *R*′, *R*″ = alkyl, aryl, alkoxyl) toward selenium acceptors can be quantified by the coupling constant $^1J(^{31}P–^{77}Se)$ [7,15]. It was found that electron-withdrawing groups at phosphorus increase $^1J(^{31}P–^{77}Se)$, due to the increased *s* character of the phosphorus orbital involved in the P–Se bonding. Furthermore, the steric demand around phosphorus causes marked changes in the behavior of the respective transition metal complexes. These features are essential parameters for the specific design of transition metal complexes. The $^1J(^{31}P–^{77}Se)$ values for seleno phosphines **4a**–**f** are summarized in Table 2. Since electronic

Table 2
Chemical shifts (ppm) of **4a**–**f**, **6e**, **6f**, **7a**–**c**, $^1J(^{31}P–^{77}Se)$ coupling constants (Hz) of **4a**–**f** and calculated Tolman cone angles Θ (°) of **6e**, **6f** and **7a**–**c**; $Ph_3P(=Se)$ and $[(Ph_3P)_2PdCl_2]$ for comparison.

Compd.	δ [ppm]	$^1J(^{31}P–^{77}Se)$ [Hz]	Compd.	δ [ppm]	Θ [°] [a]
4a	4.3	746	**6e**	49.7	183
4b	0.9	729	**6f**	31.0	177
4c	−17.5	710			
4d	−37.9	784	**7a** [6b]	5.0	168
4e	56.3	715	**7b**	−6.8	168
4f	31.0	713	**7c**	−24.0	213
Ph_3P=Se	35.9 [7]	732 [7]	**$[(PPh_3)_2PdCl_2]$**	24.5	145 [16a]

[a] Θ = Tolman cone angle calculated by STERIC [17].

and steric effects are intimately related [16], Table 2 also contains the Tolman cone angles of **6e**, **6f**, and **7a**–**c**. The Tolman cone angle Θ is the apex angle of a cylindrical cone centered 2.28 Å from the center of the phosphorus atom which touches the van-der-Waals radii of the outermost atoms [16]. Increasing the M–P–R angle between P and R decreases the percentage of the *s* character in the phosphorus lone-pair. Within our studies we replaced one substituent *R* of PR_3 by a (ferrocenylethynyl) ligand to obtain $R_2(FcC{\equiv}C)P$ (**3a**–**f**). Out of this reason, we calculated the Tolman cone angle from the structural data obtained from the single X-ray determination of **6e**, **6f**, **7a** [6b], **7b** and **7c** using the program STERIC [17] (Table 2).

From Table 2 it can be seen that substitution of *R* by a ferrocenylethynyl unit causes a shielding of the phosphorus atom with an increase of $^1J(^{31}P–^{77}Se)$ confirming that the (ferrocenylethynyl) building block is electron-withdrawing. Furthermore, the replacement of *R* by FcC≡C directly influences the Tolman cone angle Θ (for example, $P(C_6H_5)_3$ (145°) [16a]/**3a** (168°)) showing that the introduction of a FcC≡C unit increases Θ. However, for larger substituents, *i.e.* mesityl, the increase in the Tolman cone angle is less significant ($P(2,4,6\text{-}Me_3C_6H_2)_3$ (212°) [16a]/**3c** (213°)). The electronic and steric parameters can be used for the specific design of catalytic active palladium transition metal complexes, for example, for *C*,*C* coupling reactions (vide supra) which should have direct influence on the catalytic activity of the appropriate catalyst.

The redox properties of (ferrocenylethynyl)phosphines **3**, **4**, and their corresponding palladium complexes **6** and **7** were studied by cyclic voltammetry (CV), square wave voltammetry (SWV, complexes **6** and **7**), linear sweep voltammetry (LSV, **7**), and spectro–electrochemistry (*in situ* UV–Vis/NIR and IR spectroscopy, **7f**) in dry dichloromethane utilizing 0.1 mol L^{-1} solutions containing $[N^nBu_4][B(C_6F_5)_4]$ as supporting electrolyte. Tetra-^{n}butyl ammonium tetrakis(perfluorophenyl)borate was chosen because it provides close-to-optimal conditions for electrochemical experiments by minimizing nucleophilic attack by the electrolyte anion and improvement of the product solubility [18]. The cyclovoltammetric studies were carried out at scan rates of 100 mV s^{-1} and the results are summarized in Table 3. All potentials are referenced to the FcH/FcH^+ redox couple (Fc = $Fe(\eta^5\text{-}C_5H_4)(\eta^5\text{-}C_5H_5)$) as recommended by IUPAC [19].

The electrochemically most studied member of the series of (ferrocenylethynyl)phosphines **3a**–**f** is **3a** [6b], which undergoes a reversible one-electron oxidation at E^0 = 0.161 V (Table 3). As already described in literature for various phosphines, including 1,1′-bis(diphenylphosphine)ferrocene, the resulting ferrocenium ion participates in intra-molecular electron transfer from the PPh_2 group to iron. The formed phosphorus(IV) radical then reacts in different follow-up reactions, *e.g.* dimerization or reaction with traces of oxygen [20,21a]. Nevertheless, in consecutive cycles depending on the groups *R* reversible as well as irreversible oxidations occur as it is typical of ferrocenyl phosphines (Fig. 3)

Table 3
Cyclovoltammetric data (potentials *vs.* FcH/FcH^+), scan rate 100 mV s^{-1} at a glassy carbon electrode of 1.0 mmol L^{-1} solutions of **3**, **4**, **6**, and **7** in dry dichloromethane containing 0.1 mol L^{-1} of $[N^nBu_4][B(C_6F_5)_4]$ as supporting electrolyte at 25 °C.

Compd.	E^0 (ΔE_p)/*V* (V)	$E_{ox\text{-}irrev}$/*V*	$E_{red\text{-}irrev}$/*V*	Compd.	E_1^0 (ΔE_p)/*V* (V)	E_2^0 (ΔE_p)/*V* (V)	E_{irrev}/*V*	ΔE^0/*V*
3a	0.161 (0.068)			**6e**	0.204 (0.144) [a]		$E_{red} = -0.976$	
3b	0.149 (0.094)			**6f**	0.204 (0.120) [a]		$E_{red} = -0.916$	
3c		0.153	0.085					
		0.271	0.287					
		0.483	0.407					
		0.807						
3d	0.165 (0.072)	1.161	0.497	**7a**	0.630 (0.080) [b]			
3e		0.152	0.078	**7b**	0.280 (0.100)	0.374 (0.100)		0.094
		0.528	0.262					
		1.182	0.450					
3f		0.144	0.314	**7c**	0.162 (0.184) [a]			
		0.380	0.444					
		0.496						
				7d	0.301 (0.142) [a]			
4b		0.293	−0.799	**7e**	0.152 (0.140) [a]			
		0.629	−0.413					
		0.745	0.249					
			0.495					
4c		0.234	−0.616	**7f**	0.273 (78)	0.438 (0.080)		0.165
		0.578	0.270					
		0.808	0.476					
4d	0.292 (0.082)	0.529	−0.627					
			0.491					
4e		0.289	−0.355					
		0.753	0.161					
			0.603					
4f		0.286	−0.400					
		0.716	0.192					
			0.592					

[a] Two *non*-resolved Fe(II)/Fe(III) processes.
[b] Redox potential E^0 and ΔE_p from reference 6b. E^0 = redox potential, E_1^0 = potential of 1st redox process, E_2^0 = potential of 2nd redox process, $E_{ox\text{-}irrev}$ = irreversible oxidation potential, $E_{red\text{-}irrev}$ = irreversible reduction potential, ΔE_p = difference between oxidation and reduction potential, ΔE^0 = potential difference between two redox processes.

[20,21a]. Obviously, the phosphines featuring electron-rich organic groups, for example, **3c**, **3e** and **3f** show without exception irreversible behavior and more follow-up processes (Fig. 3).

From Table 3 it further can be seen that more electron-rich species can more easily be oxidized. The potential E^0 and $E_{ox\text{-}irrev}$, respectively, decreases, for example, in the series: furyl > phenyl > *o*-tolyl ≈ mesityl. The appropriate alkyl-functionalized ferrocenylethynyl phosphines show the trend *E*(*t*-butyl) > *E*(cyclohexyl) (Table 3). Compared with the corresponding ferrocenyl phosphines $PFcR_2$ [15g], the ferrocenylethynyl-functionalized derivatives are more difficult to oxidize which complies with the electron-withdrawing character of the ethynyl spacer unit. As recently described for ferrocenyl phosphines [15g], we did synthesize the seleno phosphines **4a**–**f** (vide supra) which show a similar behavior with irreversible oxidation events and follow-up reactions as ferrocenyl-substituted seleno phosphines (Table 3) [15g,18,21a]. Compared to **3a**–**f** with phosphorus III, the seleno phosphines **4a**–**f** with phosphorus in the oxidation state + V are, as expected, more difficult to oxidize (Table 3).

Coordination of the phosphorus lone-pair in **3a**–**f** to palladium (complexes **6** and **7**) inhibits intra-molecular oxidation of the phosphorus (Fig. 4).

Typical for both dimeric palladium complexes **6e** and **6f** is that in the cyclic voltammograms beside two *non*-resolved redox events

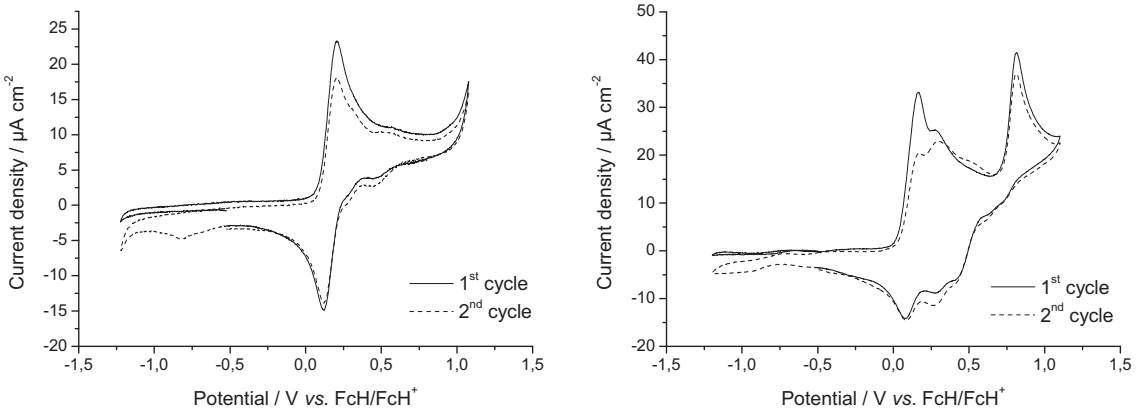

Fig. 3. Electrochemical data of dichloromethane solutions containing 1.0 mmol L^{-1} of **3a** (left) and **3c** (right) at 25 °C, supporting electrolyte $[N^nBu_4][B(C_6F_5)_4]$ with a scan rate of 100 mV s^{-1}.

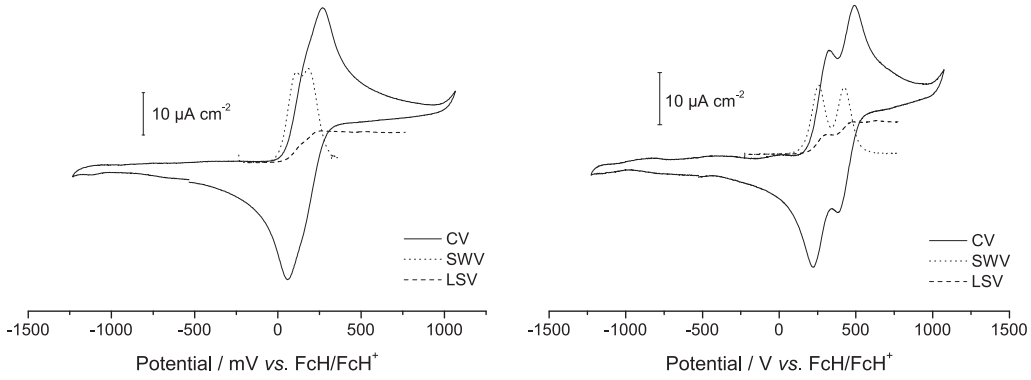

Fig. 4. Electrochemical data of dichloromethane solutions containing 1.0 mmol L^{-1} of **7c** (left) and **7f** (right) at 25 °C, supporting electrolyte $[N^nBu_4][B(C_6F_5)_4]$ with a scan rate of 100 mV s^{-1} (CV = Cyclic Voltammetry, SWV = Square Wave Voltammetry, LSV = Linear Sweep Voltammetry).

at 0.204 V ($\Delta E_p = 0.144$ V (**6e**) and $\Delta E_p = 0.120$ V (**6f**), respectively) for the oxidation of the ferrocenyl groups an irreversible reduction peak at −0.9 V associated with the reduction of Pd(II) to Pd(0) [21b,c] is observed (Supplementary Information, Figure S1; Table 3). However, mononuclear palladium complexes **7b**–**f** show two reversible redox events between 0.2 and 0.5 V, *i.e.* **7f**: $E_1^0 = 0.27$ V ($\Delta E_p = 0.078$ V), $E_2^0 = 0.44$ V ($\Delta E_p = 0.080$ V) (Table 3, Fig. 4). The same behavior is found for all other species, even though they are partially not separable. Conspicuous is the observation that aliphatic **7f** shows a larger peak separation of the 1st and 2nd oxidation than the aromatic systems **7a**–**d** (Fig. 4). Square wave (SWV) and linear sweep (LSV) voltammetric studies indicated, as exemplary shown for **7f** (Fig. 4, right), two reversible one-electron processes with a peak separation of 0.165 V. This divergent behavior shows that the two ferrocenyl moieties in **7f** can separately be oxidized rather than **7a**–**e**. As already described for **3a**–**f** and **4a**–**f**, respectively, complexes **7** show the same trend, in that the ferrocenyl groups of the more electron-rich aromatic phosphines are, as expected, easier to oxidize. Compared to the *non*-coordinated (ferrocenylethynyl)phosphines, the respective palladium complexes are also more difficult to oxidize which can be explained by electron donation of the phosphines to palladium upon coordination (Table 3). In addition, for **6** and **7** no further redox events indicating follow-up reactions have been observed.

To probe, if the redox splitting in **7f** is due to electronic communication we investigated the electronic absorptions in the visible and near infrared region of the electrochemically generated oxidized species ($\mathbf{7f}^+$, $\mathbf{7f}^{2+}$) (Fig. 5). In general, the absence of any NIR charge transfer bands points to electron-localized mixed-valent species, whereas the presence of such absorptions would argue in favor of electron delocalization. The spectro–electrochemical studies were conducted by stepwise increase of the potential from 0.0 to 1.2 V *vs.* Ag/AgCl in an OTTLE cell (OTTLE = Optically Transparent Thin-Layer Electrochemical) containing dichloromethane solutions of **7f** (1.0 mmol L^{-1}) and $[N^nBu_4][B(C_6F_5)_4]$ (0.1 mol L^{-1}) as supporting electrolyte allowing the generation of mono-cationic $[\mathbf{7f}]^+$ and di-cationic $[\mathbf{7f}]^{2+}$ species. Complex **7f** does not display, as expected, any absorption in the NIR range. Surprisingly, the spectrum of the mono-oxidized species **7f** $[\mathbf{B(C_6F_5)_4}]$ shows an absorption with relatively high intensity (Fig. 5), which is in contrast to other ferrocenyl phosphine palladium complexes, *i. e.* $[PdCl_2(P(2\text{-}CH_3C_6H_4)_2Fc)_2]$ [15g]. Nevertheless, it must be noted that during the UV–Vis/NIR measurements decomposition of the oxidized species occurred, which resulted in incomplete disappearance of the IVCT band. However, when increasing the speed of the measurement and reducing the amount of data, the IVCT band completely disappeared (Figure S2, Supplementary Information). To investigate this behavior we tried to synthesize the mono-cationic species by treatment of **7f** with one equivalent of $[Ag][B(C_6F_5)_4]$ in tetrahydrofuran at −60 °C. After filtration and precipitation with ^{n}hexane a dark purple solid could be obtained. Nevertheless, characterization of this material indicated that solely di-cationic $[\mathbf{7f}]^{2+}$ was formed. UV–Vis/NIR measurements showed no absorption in the NIR range (Supplementary Information, Figure S3).

Deconvolution of the NIR absorption of *in situ* generated $[\mathbf{7f}]^+$ was achieved by using three separate overlapping transitions with Gaussian shapes (Fig. 6). The fits provide an almost exact overlay of the sum of the Gaussian curves with the experimental spectra. Two bands were found at 6303 and 4444 cm^{-1}, respectively. The absorption possessing the highest intensity ($\mathring{a}_{max} = 1410$ L mol^{-1} cm^{-1}) at 6303 cm^{-1} showed a characteristic

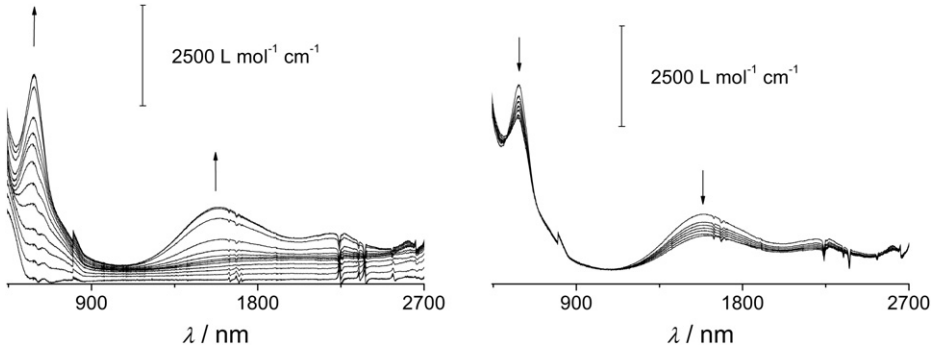

Fig. 5. NIR-Spectra of 7f at rising potentials (left: 0.0–0.775 V; right: 0.8–1.2 V *vs.* Ag/AgCl) at 25 °C, in dichloromethane, supporting electrolyte $[N^nBu_4][B(C_6F_5)_4]$.

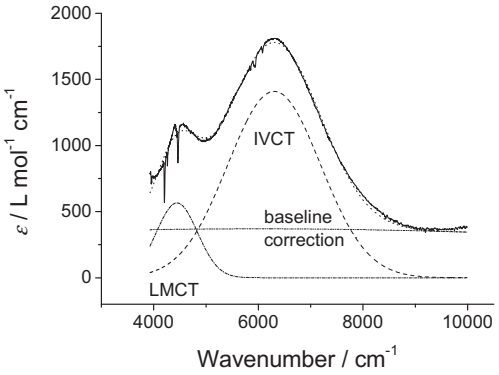

Fig. 6. Deconvolution of NIR absorptions of electro generated $[\mathbf{7f}]^+$ using three Gaussian-shaped bands. Solid line: experimental data; dashed/dotted lines: Gaussian-shaped absorptions.

peak width-at-half-height for inter-valence charge transfer bands (2089 cm^{-1}) [22]. The band at 4444 cm^{-1} can be assigned to a ligand-to-metal charge transfer absorption [23]. A 3rd Gaussian curve represents the baseline correction.

In addition, band shape analysis was performed according to the Hush model for symmetric mixed-valent species (equations (1) and (2)) [23b,24] and the classification criteria of Brunschwig, Creutz and Sutin [25].

$$\left(\Delta\nu_{\frac{1}{2}}\right)_{\text{theo}} = \sqrt{2310\cdot\nu_{\max}} \tag{1}$$

$$\Gamma = 1 - \frac{\left(\Delta\nu_{\frac{1}{2}}\right)}{\left(\Delta\nu_{\frac{1}{2}}\right)_{\text{theo}}} \tag{2}$$

Theoretical band width-at-half-height could be calculated as 3816 cm^{-1} for $[\mathbf{7f}]^+$ and a τ value of 0.45 indicates that this radical cation is rather close to a Class II/III borderline system. According to this classification, complex **7f** can be assigned as moderately coupled class II system.

Additionally, spectro–electrochemical IR measurements of **7f** were performed to confirm electronic interactions. These studies were performed by stepwise increase of the potential from −1.0 to +1.2 V in an OTTLE cell containing a dichloromethane solution of **7f** (2.5 mmol L^{-1}) and $[N^nBu_4][B(C_6F_5)_4]$ (0.1 mol L^{-1}) as supporting electrolyte. The IR spectrum of **7f** displays one strong $\nu_{C\equiv C}$ band at 2159 cm^{-1} and one very weak band at 2180 cm^{-1} which most probably can be assigned to the *trans*-complex (Fig. 7). Oxidation of **7f** to $[\mathbf{7f}]^+$ results in a shift to lower wavenumbers (2154 cm^{-1}) and the disappearance of the 2nd weak band. Further oxidation to $[\mathbf{7f}]^{2+}$ causes an additional shift (2151 cm^{-1}) and a broadening of the respective absorption. Besides, for $[\mathbf{7f}]^+$ only one absorption is observed which seems like the average of the neutral and dicationic species. However, these differences are small [26].

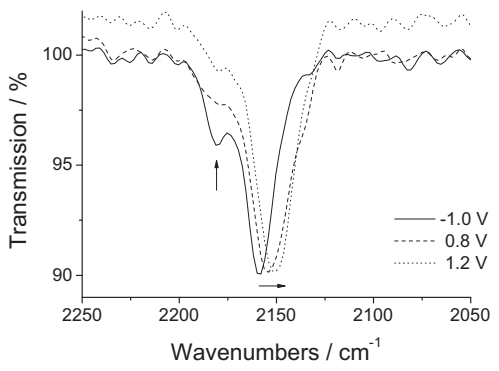

Fig. 7. IR spectra of **7f** at rising potentials (−1.0 to +1.2 V *vs.* Ag/AgCl) at 25 °C in dichloromethane, supporting electrolyte $[N^nBu_4][B(C_6F_5)_4]$.

2.1.1. C,C cross-coupling reactions

Suzuki and Heck reactions are of great interest because they allow *C,C* coupling of alkyl and aryl halides with aryl boronic acids, or aryl and alkenyl halides with α-olefines under mild conditions, providing a convenient access to biaryls and diverse alkenes [9]. These couplings are one of the most powerful C^2_{sp}–C^2_{sp} bond forming reactions in organic and organometallic synthesis. Next to *N*-heterocyclic carbenes [11] and phosphapalladacycles [13] *etc.*, phosphines remain among the best studied ligands in such reactions [10].

2.1.2. Suzuki reaction

In recent years, manifold and efficient synthetic methodologies were developed to synthesize specifically designed phosphine ligands for the homogeneous palladium-catalyzed Suzuki cross-coupling reaction [9]. Contrary, transition metal-containing phosphines are only little described of which dppf (=1,1′-bis(diphenylphosphino)ferrocene) and derivatives thereof have been best investigated [10f]. With this study we enrich the family of ferrocenyl phosphine palladium dichloride complexes and describe their use as catalysts in the Suzuki reaction. The reactants 2-bromo toluene and 4′-chloro acetophenone, respectively, of the catalytic process were treated with phenyl boronic acid in presence of potassium carbonate in a 2:1 (*v*/*v*) mixture of dioxane/water (Reaction 2). The reaction mixture was stirred at 100 °C for 1 h, samples were taken after defined periods of time (Experimental Section). Acetyl ferrocene was added as internal standard for ^1H NMR analysis to determine the conversions of the catalytic reactions. Palladium complexes **6** and **7** were applied in the catalytic reaction of 2-bromo toluene with phenyl boronic acid (Fig. 8, left). From these studies the most promising candidates were additionally used in the coupling of 4′-chloro acetophenone with phenyl boronic acid (Fig. 8, right).

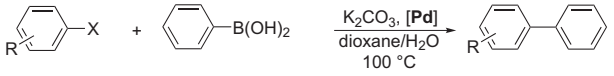

R = 2-CH_3 , X = Br
R = 4-$COCH_3$, X = Cl

In the Suzuki reaction electron-rich phosphine ligands are best suited [10a,b], which correlates with our results (Fig. 8). From Fig. 8 it further can be seen that quantitative conversions are obtained for the reaction of 2-bromo toluene with phenyl boronic acid using **6** and **7** as catalyst, except **7c** (54% conversion) and **7d** (87% conversion), respectively. At first glance this is surprising but considering the Tolman cone angles (**7c**, 212°; vide supra) in a certain manner it is comprehensible. Complex **7d** features with its furyl groups electron-withdrawing substituents and hence shows the lowest catalytic activity and needs an induction period of ca. 10 min. From these studies we chose complexes **6e**, **6f**, **7e** and **7f** as catalysts for the activation of 4′-chloro acetophenone. These results are depicted in Fig. 8 (right). The highest catalytic activity is observed for **6e** and **7f**, whereas complete conversion is only observed for **6e**. A clear

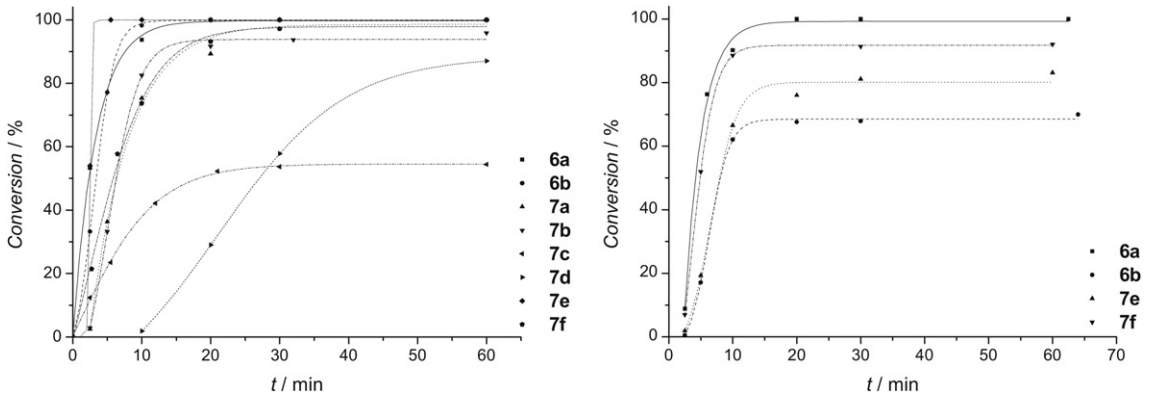

Fig. 8. Reaction profiles for the coupling of 2-bromo toluene (left) and 4′-chloro acetophenone (right) (2.92 or 3.0 mmol) with phenyl boronic acid (3.85 mmol) using **6e**, b and **7a**–**f** as catalysts (catalyst loading 0.25 (2-bromo toluene) and 0.5 mol% (4′-chloro acetophenone), 100 °C, 1 h, K_2CO_3 (8.76 mmol) in a mixture of dioxane/water (ratio 2:1, *v*/*v*) (10 mL)).

trend between dimeric **6** and monomeric **7** cannot be seen. Compared to ferrocenyl phosphine palladium dichloride complexes of type $[PdCl_2(PR_2Fc)_2]$ (Fc = Fe(η^5-C_5H_4)(η^5-C_5H_5)) [15g] and up-to-date used catalyic systems [9–13] they show, however, a lower activity and productivity.

2.1.3. Heck reaction

The palladium-promoted Heck *C*,*C* cross-coupling between aryl- or vinyl halides and triflates and alkenes in the presence of a base allows the straightforward synthesis of C_{sp2}–C_{sp2} single bonds for fine chemical synthesis [9]. One advantage of the Heck reaction is its *trans* selectivity. As catalysts, for example, phosphapalladacycles [13], various palladium(II)–acetate/phosphine systems [9], palladium nanoparticles [27], and *N*-heterocyclic carbene palladium complexes [11] have been applied. Within this work, complexes **6e**, **6f**, and **7a**–**f** were used in the coupling of iodo benzene with *tert*-butyl acrylate (Reaction 3) in a mixture of toluene–acetonitrile (ratio 1:1, *v*:*v*) in presence of NEt^iPr_2 at 80 °C with a catalyst loading of 0.5 mol% (Experimental Section, Table 4).

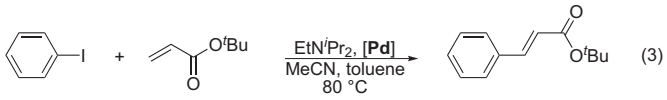

(3)

From Table 4 it can be seen that the catalyst featuring sterically demanding tolyl (**7b**) and mesityl phosphines (**7c**), or weekly σ-donating furyl ligands (**7d**) are best suited for *C*,*C* couplings under the above mentioned conditions. However, with these species quantitative conversion could not be reached. Complexes **6e**, **6f**, and **7a** with aliphatic (**6e**, **b**) or less bulky and electron-poor phosphines show lesser activity and productivity as compared with **7b**, **7c**, and **7d**. It is obvious that dimeric **6e** and **6f** are only active at the beginning of the reaction but significantly slowed down in activity due to their lower stability, when compared to **7a**–**f** (Supplementary Information, Figure S4). Based on these results, we did not consider the reactions of bromo or chloro benzene with *tert*-butyl acrylate supported by catalysts **6** and **7** since smaller conversions and longer reaction times are expected. In contrast to now-a-days used catalysts [11f,12d,28] our systems are less active and productive. Compared to ferrocenyl phosphine palladium catalysts the appropriate (ferrocenylethynyl) complexes possess lower activity attributed to the electron-withdrawing effect of the ethynyl linker unit.

Table 4
Heck reaction of iodo benzene with *tert*-butyl acrylate with a catalyst loading of 0.5 mol% of **6** and **7**, 10 h reaction time.

Entry	Compd.	Yield/%	Entry	Compd.	Yield/%
1	**6e**	27.1	5	**7c**	41.9
2	**6f**	41.2	6	**7d**	52.9
3	**7a**	41.9	7	**7e**	3.8
4	**7b**	61.9	8	**7f**	21.4

3. Conclusions

Within this study the synthesis of a series of (ferrocenylethynyl) phosphine palladium dichloride complexes of type $[Pd(Cl)(\mu\text{-}Cl)(P(C{\equiv}CFc)R_2)]_2$ (Fc = Fe(η^5-C_5H_4)(η^5-C_5H_5); $R = {}^t$Bu, $^cC_6H_{11}$) and $[PdCl_2(P(C{\equiv}CFc)R_2)_2]$ ($R = C_6H_5$, 2-MeC_6H_4, 2,4,6-$Me_3C_6H_2$, $^cC_4H_3O$, ^{t}Bu, $^cC_6H_{11}$) by the reaction of $P(C{\equiv}CFc)R_2$ with $[PdCl_2(cod)]$ (cod = cyclo-1,5-octadiene) or $[PdCl_2(SEt_2)_2]$ is discussed. The structures of four complexes could be determined by single crystal X-ray diffraction analysis. $[PdCl_2(P(C{\equiv}CFc)(2\text{-}MeC_6H_4)_2)_2]$ shows in the solid state a *cis*-configuration, whereas $[PdCl_2(P(C{\equiv}CFc)(2,4,6\text{-}Me_3C_6H_2)_2)_2]$ prefers the *trans*-form with linear FcC≡CP moieties. In contrast, $[Pd(Cl)(\mu\text{-}Cl)(P(C{\equiv}CFc)(^tBu)_2)]_2$ and $[Pd(Cl)(\mu\text{-}Cl)(P(C{\equiv}CFc)(^cC_6H_{11})_2)]_2$ form dimers with a planar $Pd_2P_2Cl_2(\mu\text{-}Cl)_2$ core with the (ferrocenylethynyl) ligands oriented above and below the square-planar unit. For classification of the σ-donor ability of the (ferrocenylethynyl)phosphines the respective seleno derivatives $(Se)P(C{\equiv}CFc)R_2$ have been synthesized upon addition of selenium in its elemental form to the (ferrocenylethynyl)phosphines. High $^1J(^{31}P{-}^{77}Se)$ values indicate electron-poor phosphines and hence less donor capability [7,15]. Cyclovoltammetric measurements showed that depending on the groups *R* reversible as well as irreversible oxidations occur. The oxidation at the iron center leads to an intra-molecular electron transfer process from the phosphino group to iron resulting in irreversible oxidations which lead to various follow-up processes [20,21a]. We also investigated the electrochemistry of the newly synthesized seleno phosphines and (ferrocenylethynyl)phosphine palladium(II) complexes in which the lone-pair of electrons at phosphorus is part of a phosphorus–selenium or phosphorus–palladium bond. Nevertheless, the seleno phosphines also show follow-up processes, presumably resulting from an intra-molecular electron transfer from the selenium-centered radical [15g,18,21]. Such oxidations are, however, inhibited, when the phosphorus atom is datively-bonded to Pd as implemented in the respective transition metal complexes. As expected, the phosphino palladium species are more difficult to oxidize because of electron donation to Pd(II). Complex $[PdCl_2(P(C{\equiv}CFc)(^cC_6H_{11})_2)_2]$ revealed two reversible one-electron processes with a peak separation of $\Delta E^0 = 0.165$ V in

dichloromethane and in the presence of $[N^nBu_4][B(C_6F_5)_4]$ as supporting electrolyte. *In situ* UV–Vis/NIR spectroscopy confirmed moderate electronic coupling between the (ferrocenylethynyl) units and the complex can be classified as class II system according to Robin and Day [29] by band shape analysis of the IVCT absorption. Due to the long "through bond" electron transfer distance between the end-grafted ferrocenyl moieties we suppose that communication occurs rather "through space" than "through bond". Additional *in situ* IR measurements showed a small shift in the $\nu_{C\equiv C}$ band which underlines the supposition of "through space" electronic coupling.

All (ferrocenylethynyl)phosphine palladium(II) complexes were tested as catalysts in *C,C* coupling reactions. In the palladium-promoted Heck reaction, iodo benzene was treated with *tert*-butyl acrylate. All complexes are active, although the most efficient catalysts were the ones featuring furyl, mesityl or *o*-tolyl substituted phosphines explainable either by the bulkiness (Tolman cone angle) or the weak σ-donor ability ($^1J(^{31}P-^{77}Se)$) of these ligands. Furthermore, it could be shown that all Pd species are active in Suzuki couplings of aryl-bromide and activated aryl–chloride with phenyl boronic acid. A relation between the basicity of the phosphines and the activity of the corresponding complexes exists. The lower the $^1J(^{31}P-^{77}Se)$ coupling constant and hence the higher the basicity of the phosphine, the higher the catalyst activity. However, the catalysts reported within this work are compared with up-to-date catalytic systems [9–13,15g,28] less active.

4. Experimental section

4.1. General data and materials

All reactions were carried out under an atmosphere of nitrogen or argon using standard Schlenk techniques. Toluene and diethyl ether were purified by distillation from sodium/benzophenone, dichloromethane was purified by distillation from calcium hydride. Celite (purified and annealed, Erg. B.6, Riedel de Haen) was used for filtrations. For column chromatography alumina with a particle size of 90 μm (standard, Merck KGaA) or silica with a particle size of 40–60 μm (230–400 mesh (ASTM), Becker) was used. All starting materials were obtained from commercial suppliers and were used without further purification. Ethynylferrocene [30] (**1**), (ethynylferrocenyl)diphenyl phosphine [6b] (**3a**), (ethynylferrocenyl) diphenyl seleno phosphine [7] (**4a**) and bis((ethynylferrocenyl) diphenylphosphino)palladiumdichloride [6b] (**7a**) were prepared according to published procedures. Chlorophosphines **2b–f** [31], $[PdCl_2(cod)]$ [32] (**5**) and $[PdCl_2(SEt_2)_2]$ [33] (**8**) were synthesized as described in literature.

4.2. Instruments

NMR spectra were recorded on a Bruker Avance III 500 spectrometer (500.3 MHz for ^1H, 125.7 MHz for $^{13}C\{^1H\}$, and 202.5 MHz for $^{31}P\{^1H\}$ NMR spectra). Chemical shifts are reported in δ units (parts per million) downfield from tetramethylsilane with the solvent as reference signal (^1H NMR: standard internal $CDCl_3$, δ 7.26 or CD_2Cl_2, δ 5.30; $^{13}C\{^1H\}$ NMR: standard internal $CDCl_3$, δ 77.16 or CD_2Cl_2, δ 53.52; $^{31}P\{^1H\}$ NMR: standard external rel. 85% H_3PO_4, δ 0.0 or $P(OMe)_3$, δ 139.0, respectively). HRMS were recorded on a Bruker Daltonik micrOTOF-QII spectrometer (ESI-TOF). Elemental analyses were measured with a Thermo FlashAE 1112 series instrument. Melting points of analytical pure samples were determined by a Gallenkamp MFB 595 010 M melting point apparatus. FT IR spectra were recorded on a Thermo Nicolet IR 200 spectrometer using either KBr pellets or NaCl plates.

4.3. Electrochemistry

Measurements on 1.0 mmol L^{-1} solutions of **3**, **4**, **6** and **7** in dry degassed dichloromethane containing 0.1 mol L^{-1} of $[N^nBu_4][B(C_6F_5)_4]$ as supporting electrolyte were conducted under a blanket of purified argon at 25 °C utilizing a Radiometer Voltalab PGZ 100 electrochemical workstation interfaced with a personal computer. A three electrode cell, which utilized a Pt auxiliary electrode, a glassy carbon working electrode (surface area 0.031 cm^2) and an Ag/Ag^+ (0.01 mol L^{-1} $[AgNO_3]$) reference electrode mounted on a luggin capillary was used. The working electrode was pre-treated by polishing on a Buehler microcloth first with 1 micron and then ¼ micron diamond paste. The reference electrode was constructed from a silver wire inserted into a solution of 0.01 mol L^{-1} $[AgNO_3]$ and 0.1 mol L^{-1} $[N^nBu_4][B(C_6F_5)_4]$ in acetonitrile, in a luggin capillary with a vycor tip. This luggin capillary was inserted into a second luggin capillary with vycor tip filled with a 0.1 mol L^{-1} $[N^nBu_4][B(C_6F_5)_4]$ solution in dichloromethane. Successive experiments under the same experimental conditions showed that all formal reduction and oxidation potentials were reproducible within 10 mV. Experimentally potentials were referenced against an Ag/Ag^+ reference electrode but results are presented referenced against ferrocene as an internal standard as required by IUPAC [19]. Data were manipulated on a Microsoft Excel worksheet to set the formal reduction potentials of the FcH/FcH^+ couple to 0.0 V. Under our conditions the FcH/FcH^+ couple was at 230 mV *vs.* Ag/Ag^+.

4.4. Spectro–electrochemistry

Spectro–electrochemical UV/Vis-NIR measurements of a 1.0 mmol L^{-1} solution of **7f** in dry degassed dichloromethane containing 0.1 mol L^{-1} of $[N^nBu_4][B(C_6F_5)_4]$ as supporting electrolyte were carried in an OTTLE cell [34] using a Varian Cary 5000 spectrometer. *In situ* spectro–electrochemical IR measurements of **7f** (2.5 mmol L^{-1}) in dichloromethane (0.1 mol L^{-1} $[N^nBu_4][B(C_6F_5)_4]$) were also carried in an OTTLE cell [34] using a Thermo IR 100 spectrometer.

4.5. General procedure for the synthesis of phosphines *3b–f*

To a solution of **1** dissolved in 50 mL of dry diethyl ether one equivalent of a 2.5 M solution of ^{n}BuLi was added dropwise at −30 °C. After stirring the solution for 30 min at ambient temperature it was again cooled to −30 °C and one equivalent of the appropriate chlorophosphine **2** was added dropwise. The reaction mixture was stirred for 1 h at ambient temperature and then concentrated in vacuum. The resulting residue was purified by column chromatography (column size: 15 × 3.0 cm) and dried in vacuum.

4.5.1. Synthesis of $P(C\equiv CFc)(2\text{-}MeC_6H_4)_2$ (*3b*)

Using the general procedure described above, 1.0 g (4.76 mmol) of **1** was reacted with 1.90 mL (4.75 mmol) of ^{n}BuLi and then 1.18 g (4.75 mmol) of chlorodi-*o*-tolylphosphine (**2b**) was added in a single portion. The resulting residue was purified by column chromatography on alox using a mixture of ^{n}hexane/diethyl ether (ratio 20:1, *v*:*v*) as eluent. Phosphine **3b** was obtained as a yellow solid. Yield: 1.33 g (3.15 mmol, 66% based on **2b**). Anal. Calcd. for $C_{26}H_{23}FeP$ (422.28 g/mol): C, 73.95; H, 5.49. Found: C, 73.71; H, 5.23. Mp.: 118 °C. IR (KBr, ν/cm^{-1}): 745 (s, =C–H, *ortho*-disubst. benzene), 1449 (m, P–C), 2150 (m, C≡C), 2913/2937/2966 (w, C–H), 3059/3083 (w, =C–H). ^1H NMR (500.30 MHz, $CDCl_3$, δ): 2.52 (s, 6 H, 2-$CH_3C_6H_4$), 4.22 (s, 5 H, C_5H_5), 4.24 (pt, $^3J_{HH}$ = 1.9 Hz, 2 H, C_5H_4), 4.52 (pt, $^3J_{HH}$ = 1.9 Hz, 2 H, C_5H_4), 7.20–7.26 (m, 4 H, 2-

$CH_3C_6H_4$), 7.28–7.34 (m, 2 H, 2-$CH_3C_6H_4$), 7.56–7.62 (m, 2 H, 2-$CH_3C_6H_4$). $^{13}C\{^1H\}$ NMR (125.81 MHz, $CDCl_3$, δ): 21.3 (d, $^3J_{CP}$ = 20.6 Hz, 2-$CH_3C_6H_4$), 69.2 (m, C^{β}/C_5H_4), 70.1 (s, C_5H_5), 72.0 (d, $^2J_{CP}$ = 1.6 Hz, C^{α}/C_5H_4), 81.1 (d, $^2J_{CP}$ = 3.9 Hz, $-C{\equiv}C-P$), 107.7 (d, $^1J_{CP}$ = 5.5 Hz, $-C{\equiv}C-P$), 126.3 (d, J_{CP} = 2.2 Hz, 2-$CH_3C_6H_4$), 129.3 (s, 2-$CH_3C_6H_4$), 130.3 (d, J_{CP} = 5.1 Hz, 2-$CH_3C_6H_4$), 133.0 (d, J_{CP} = 3.4 Hz, 2-$CH_3C_6H_4$), 133.7 (d, J_{CP} = 6.4 Hz, 2-$CH_3C_6H_4$), 142.0 (d, J_{CP} = 26.6 Hz, 2-$CH_3C_6H_4$). $^{31}P\{^1H\}$ NMR (202.53 MHz, $CDCl_3$, δ): −47.7. HRMS (ESI-TOF) $C_{26}H_{23}FeP$ $[M + nH]^+$ m/z: calcd.: 423.0960, found: 423.0963.

4.5.2. Synthesis of P(C≡CFc)(2,4,6-Me$_3$C$_6$H$_4$)$_2$ (3c)

Using the general procedure described above, 1.0 g (4.76 mmol) of **1** was reacted with 1.90 mL (4.75 mmol) of ^{n}BuLi and then with 1.45 g (4.75 mmol) of chlorodimesitylphosphine (**2c**). The resulting residue was purified by column chromatography on silica gel using ^{n}hexane/diethyl ether (ratio 15:1, *v*:*v*) as eluent. Compound **3c** was obtained as a yellow solid. Yield: 1.82 g (3.80 mmol, 80% based on **2c**). Anal. Calcd. for $C_{30}H_{31}FeP$ (478.39 g/mol): C, 75.32; H, 6.53. Found: C, 75.27; H, 6.63. Mp.: 113 °C. IR (KBr, ν/cm^{-1}): 820 (s, =C–H, *para*-subst. benzene), 1449/1467 (m, P–C), 1598 (m, C=C), 2140 (m, C≡C), 2919/2954 (m, C–H), 3096 (w, =C–H). ^1H NMR (500.30 MHz, $CDCl_3$, δ): 2.28 (s, 6 H, 2,4,6-(CH_3)$_3$C$_6$H$_2$), 2.47 (s, 12 H, 2,4,6-(CH_3)$_3$C$_6$H$_2$), 4.16 (s, 5 H, C_5H_5), 4.20 (pt, $^3J_{HH}$ = 1.8 Hz, 2 H, C_5H_4), 4.41 (pt, $^3J_{HH}$ = 1.8 Hz, 2 H, C_5H_4), 6.84 (d, $^4J_{HP}$ = 3.1 Hz, 4 H, 2,4,6-(CH_3)$_3$C$_6H_2$). $^{13}C\{^1H\}$ NMR (125.81 MHz, $CDCl_3$, δ): 21.0 (s, 2,4,6-(CH_3)$_3$C$_6$H$_2$), 23.2 (d, $^3J_{CP}$ = 14.3 Hz, 2,4,6-(CH_3)$_3$C$_6$H$_2$), 65.8 (m, C^i/C_5H_4), 68.9 (s, C^{β}/C_5H_4), 69.7 (s, C_5H_5), 71.4 (d, $^4J_{CP}$ = 1.6 Hz, C^{α}/C_5H_4), 83.4 (d, $^2J_{CP}$ = 2.9 Hz, $C{\equiv}C-P$), 106.2 (d, $^1J_{CP}$ = 9.4 Hz, $C{\equiv}C-P$), 130.0 (d, $^3J_{CP}$ = 3.6 Hz, C^m/2,4,6-(CH_3)$_3$C$_6$H$_2$), 130.4 (d, $^1J_{CP}$ = 12.6 Hz, C^i/2,4,6-(CH_3)$_3$C$_6$H$_2$), 138.2 (s, C^p/2,4,6-(CH_3)$_3$C$_6$H$_2$), 142.0 (d, $^2J_{CP}$ = 15.8 Hz, C*o*/2,4,6-(CH_3)$_3$C$_6$H$_2$). $^{31}P\{^1H\}$ NMR (202.53 MHz, $CDCl_3$, δ): −55.7. HRMS (ESI-TOF) $C_{30}H_{31}PFe$ $[M]^+$ m/z: calcd.: 478.1508, found: 478.1507.

4.5.3. Synthesis of P(C≡CFc)(^{c}C$_4$H$_3$O)$_2$ (3d)

Using the general procedure described above, 1.0 g (4.76 mmol) of **1** was reacted with 1.90 mL (4.75 mmol) of ^{n}BuLi and then with 0.95 g (4.74 mmol) of chlorodi-2-furylphosphine (**2d**). The resulting residue was purified by column chromatography on alox using ^{n}hexane as eluent giving **3c** as a yellow solid. Yield: 1.37 g (3.66 mmol, 77% based on **2d**). Anal. Calcd. for $C_{20}H_{15}FeO_2P$ (374.15 g/mol): C, 64.20; H, 4.04. Found: C, 64.33; H, 4.04. Mp.: 110 °C. IR (KBr, ν/cm^{-1}): 1010 (s, C–O), 1458 (m, P–C), 1655 (w, C=C), 2153 (m, C≡C), 3114/3142 (w, =C–H). ^1H NMR (500.30 MHz, $CDCl_3$, δ): 4.19 (s, 5 H, C_5H_5), 4.22 (pt, $^3J_{HH}$ = 1.9 Hz, C_5H_4), 4.50 (pt, $^3J_{HH}$ = 1.9 Hz, C_5H_4), 6.44 (dt, $^4J_{HP}$ = 1.8 Hz, $^3J_{HH}$ = 3.3 Hz, $^3J_{HH}$ = 1.8 Hz, 2 H, H^4/C_4H_3O), 6.90 (m, 2 H, H^3/C_4H_3O), 7.67 (m, 2 H, H^5/C_4H_3O). $^{13}C\{^1H\}$ NMR (125.81 MHz, $CDCl_3$, δ): 70.4 (m, C_5H_4), 70.6 (s, C_5H_5), 72.6 (m, C_5H_4), 111.9 (pt, $^3J_{CP}$ = 4.9 Hz, C^4/C_4H_3O), 125.2 (d, $^2J_{CP}$ = 24.8 Hz, C^3/C_4H_3O), 140.9 (d, $^1J_{CP}$ = 99.3 Hz, C^2/C_4H_3O), 148.8 (d, $^4J_{CP}$ = 2.9 Hz, C^5/C_4H_3O). $^{31}P\{^1H\}$ NMR (202.53 MHz, $CDCl_3$, δ): −83.4. HRMS (ESI-TOF) $C_{20}H_{15}FeO_2P$ $[M]^+$ m/z: calcd.: 374.0154, found: 374.0053; $[M + nK]^+$ m/z: calcd.: 412.9791, found: 412.9884. The ^{13}C signals for the ethynyl functionality could not be observed.

4.5.4. Synthesis of P(C≡CFc)(^{t}Bu)$_2$ (3e)

1.0 g (4.76 mmol) of **1** was reacted according to the general synthesis methodology described earlier with 1.90 mL (4.75 mmol) of ^{n}BuLi and 0.86 g (4.75 mmol) of chlorodi-*t*-butylphosphine (**2e**). The resulting residue was purified by column chromatography on silica gel using ^{n}hexane as eluent. Compound **3e** was obtained as a yellow solid. Yield: 1.03 g (2.90 mmol, 61% based on **2e**). Anal. Calcd. for $C_{20}H_{27}FeP$ (354.25 g/mol): C, 67.81; H, 7.68. Found: C, 67.92; H, 7.85. Mp.: 121 °C. IR (KBr, ν/cm^{-1}): 1467 (m, P–C), 1653 (w, C=C), 2364 (s, C≡C), 2859/2954 (s, C–H), 3099 (w, =C–H). ^1H NMR (500.30 MHz, $CDCl_3$, δ): 1.29 (d, $^3J_{HP}$ = 12.5 Hz, 18 H, C(CH_3)$_3$), 4.20 (pt, $^3J_{HH}$ = 1.9 Hz, C_5H_4), 4.23 (s, 5 H, C_5H_5), 4.46 (pt, $^3J_{HH}$ = 1.9 Hz, C_5H_4). $^{13}C\{^1H\}$ NMR (125.81 MHz, $CDCl_3$, δ): 29.8 (d, $^2J_{CP}$ = 14.4 Hz. C(CH_3)$_3$), 32.7 (d, $^1J_{CP}$ = 16.3 Hz, $C(CH_3)_3$), 69.9 (s, C_5H_5), 70.2 (m, C^{α}/C_5H_4), 71.8 (d, $^3J_{CP}$ = 0.9 Hz, C^{β}/C_5H_5), 83.9 (d, $^1J_{CP}$ = 18.0 Hz, -C≡C–P), 104.8 (d, $^2J_{CP}$ = 2.2 Hz, -C≡C–P). $^{31}P\{^1H\}$ NMR (202.53 MHz, $CDCl_3$, δ): 10.9. HRMS (ESI-TOF) $C_{20}H_{27}FeP$ $[M + nH]^+$ m/z: calcd.: 354.1194, found: 355.1152.

4.5.5. Synthesis of P(C≡CFc)(^{c}C$_6$H$_{11}$)$_2$ (3f)

1.0 g (4.76 mmol) of **1** was reacted (general synthesis procedure see earlier) with 1.90 mL (4.75 mmol) of ^{n}BuLi followed by addition of 1.10 g (4.73 mmol) of chlorodicyclohexylphosphine (**2f**). The resulting residue was purified by column chromatography on silica gel using ^{n}hexane as eluent. Phosphine **3f** was obtained as a yellow solid. Yield: 1.71 g (4.21 mmol, 89% based on **2f**). Anal. Calcd. for $C_{24}H_{31}FeP$ (406.32 g/mol): C, 70.94; H, 7.69. Found: C, 70.48; H, 7.77. Mp.: 77 °C. IR (KBr, ν/cm^{-1}): 1444 (m, P–C), 1657 (w, C=C), 2146 (m, C≡C), 2847/2923 (s, C–H). 3095 (w, =C–H). ^1H NMR (500.30 MHz, $CDCl_3$, δ): 1.25–1.44 (m, 10 H, C_6H_{11}), 1.71–1.84 (m, 10 H, C_6H_{11}), 1.97–2.02 (m, 2 H, H_1/C_6H_{11}), 4.21 (pt, $^3J_{HH}$ = 1.8 Hz, 2 H, C_5H_4), 4.22 (s, 5 H, C_5H_5), 4.47 (pt, $^3J_{HH}$ = 1.8 Hz, 2 H, C_5H_4). $^{13}C\{^1H\}$ NMR (125.81 MHz, $CDCl_3$, δ): 26.4 (s, C_6H_{11}), 26.8 (d, J_{CP} = 18.2 Hz, C_6H_{11}), 26.9 (d, J_{CP} = 1.9 Hz, C_6H_{11}), 29.2 (d, J_{CP} = 4.5 Hz, C_6H_{11}), 30.0 (d, J_{CP} = 18.1 Hz, C_6H_{11}), 32.9 (d, $^1J_{CP}$ = 8.2 Hz, C^1/C_6H_{11}), 65.2 (s, C^i/C_5H_4), 68.6 (s, C_5H_4), 69.9 (s, C_5H_5), 71.6 (s, C_5H_4), 82.5 (d, $^1J_{CP}$ = 20.1 Hz, -C≡C–P), 104.4 (d, $^2J_{CP}$ = 2.3 Hz, $-C{\equiv}C-P$). $^{31}P\{^1H\}$ NMR (202.53 MHz, $CDCl_3$, δ): −22.1. HRMS (ESI-TOF) $C_{24}H_{31}FeP$ $[M + nH]^+$ m/z: calcd.: 407.1586, found: 407.1571.

4.6. General procedure for the synthesis of seleno phosphines 4b–f

To a toluene solution (20 mL) containing 100 mg of the respective phosphine **3b**–**f**, 1.2 equivalents of elemental selenium were added in a single portion and the reaction mixture was stirred for 1 h at 100 °C. After cooling the reaction mixture to ambient temperature, it was filtered through a pad of Celite. All volatiles were removed in vacuum giving the appropriate compounds.

4.6.1. Synthesis of (Se)P(C≡CFc)(2-MeC$_6$H$_4$)$_2$ (4b)

100 mg (0.24 mmol) of **3b** were reacted with 22 mg (0.28 mmol) of elemental selenium. After appropriate work-up, **4b** was obtained as a yellow solid. Yield: 120 mg (0.24 mmol, 100% based on **3b**). Anal. Calcd. for $C_{26}H_{23}FePSe$ (501.24 g/mol): C, 62.30; H, 4.63. Found: C, 62.12; H, 4.83. Mp.: 64 °C. IR (KBr, ν/cm^{-1}): 556 (m, P–Se), 1450 (m, P–C), 2155 (s, C≡C), 2922/2961 (w, C–H), 3055 (w, =C–H). ^1H NMR (500.30 MHz, $CDCl_3$, δ): 2.29 (s, 6 H, 2-$CH_3C_6H_4$), 4.23 (s, 5 H, C_5H_5), 4.32 (pt, $^3J_{HH}$ = 1.8 Hz, 2 H, C_5H_4), 4.58 (pt, $^3J_{HH}$ = 1.8 Hz, 2 H, C_5H_4), 7.17–7.20 (m, 2 H, H^p/2-$CH_3C_6H_4$), 7.38–7.45 (m, 4 H, H^m/2-$CH_3C_6H_4$), 8.38–8.43 (m, 4 H, H*o*/2-$CH_3C_6H_4$). ^{c}21.3 (d, $^3J_{CP}$ = 5.7 Hz, 2-$CH_3C_6H_4$), 61.1 (d, $^3J_{CP}$ = 4.1 Hz, C^i/C_5H_4), 70.2 (s, C_5H_5), 70.3 (s, C_5H_4), 72.4 (s, C_5H_4), 76.7 (d, $^1J_{CP}$ = 148.9 Hz, $-C{\equiv}C-P$), 108.8 (d, $^2J_{CP}$ = 26.3 Hz, $-C{\equiv}C-P$), 126.4 (d, J_{CP} = 14.7 Hz, 2-$CH_3C_6H_4$), 129.4 (d, J_{CP} = 85.5 Hz, 2-$CH_3C_6H_4$), 132.1 (d, J_{CP} = 11.1 Hz, 2-$CH_3C_6H_4$), 132.2 (d, J_{CP} = 3.0 Hz, 2-$CH_3C_6H_4$), 133.8 (d, J_{CP} = 15.2 Hz, 2-$CH_3C_6H_4$), 140.5 (d, J_{CP} = 9.7 Hz, 2-$CH_3C_6H_4$). $^{31}P\{^1H\}$ NMR (202.53 MHz, $CDCl_3$, δ): 0.9 ($^1J_{PSe}$ = 728.7 Hz). HRMS (ESI-TOF) $C_{26}H_{23}FePSe$ $[M + nNa]^+$ m/z: calcd.: 524.9946, found: 524.9946; $[M + nK]^+$ m/z: calcd.: 540.9686, found: 540.9665.

*4.6.2. Synthesis of (Se)P(C≡CFc)(2,4,6-$Me_3C_6H_4$)$_2$ (**4c**)*

100 mg (0.21 mmol) of **3c** were reacted with 20 mg (0.25 mmol) of elemental selenium. After appropriate work-up, **4c** was obtained as an orange solid. Yield: 117 mg (0.21 mmol, 100% based on **3c**). Anal. Calcd. for $C_{30}H_{31}FePSe$ (557.35 g/mol): C, 64.65; H, 5.61. Found: C, 64.91; H, 5.22. Mp.: 165 °C. IR (KBr, ν/cm^{-1}): 563 (m, P–Se), 821 (m, =C–H, *para*-subst. benzene), 1448 (m, P–C), 2157 (s, C≡C), 2924/2963 (m, C–H), 3021/3098 (w, =C–H). ^{1}H NMR (500.30 MHz, $CDCl_3$, δ): 2.28 (s, 6 H, 2,4,6-(CH_3)$_3$C$_6$H$_2$), 2.61 (s, 12 H, 2,4,6-(CH_3)$_3$C$_6$H$_2$), 4.18 (s, 5 H, C$_5H_5$), 4.27 (pt, $^3J_{HH}$ = 1.9 Hz, 2 H, H$^\beta$/C$_5H_4$), 4.49 (pt, $^3J_{HH}$ = 1.9 Hz, 2 H, H$^\alpha$/C$_5H_4$), 6.85 (dd, $^4J_{HP}$ = 5.2 Hz, $^4J_{HH}$ = 0.4 Hz, 4 H, 2,4,6–(CH_3)$_3$C$_6H_2$); ^{13}C{^{1}H} NMR (125.81 MHz, $CDCl_3$, δ): 21.9 (d, $^5J_{CP}$ = 1.5 Hz, 2,4,6-(CH_3)$_3$C$_6$H$_2$), 23.2 (d, $^3J_{CP}$ = 6.9 Hz, 2,4,6-(CH_3)$_3$C$_6$H$_2$), 62.2 (d, $^3J_{CP}$ = 4.5 Hz, C^i/C$_5$H$_4$), 69.9 (s, C$^\beta$/C$_5$H$_4$), 69.9 (s, C$_5$H$_5$), 71.9 (d, $^4J_{CP}$ = 1.4 Hz, C$^\alpha$/C$_5$H$_4$), 81.0 (d, $^1J_{CP}$ = 143.7 Hz, –C≡C–P), 107.3 (d, $^2J_{CP}$ = 26.8 Hz, –C≡C–P), 128.4 (d, $^1J_{CP}$ = 86.1 Hz, C/2,4,6-(CH_3)$_3$C$_6$H$_2$), 131.8 (d, J_{CP} = 11.6 Hz, C/2,4,6-(CH_3)$_3$C$_6$H$_2$), 140.5 (d, J_{CP} = 10.9 Hz, C/2,4,6-(CH_3)$_3$C$_6$H$_2$), 140.6 (d, J_{CP} = 2.4 Hz, C/2,4,6-(CH_3)$_3$C$_6$H$_2$); ^{31}P{^{1}H} NMR (202.53 MHz, $CDCl_3$, δ): –17.5 ($^1J_{PSe}$ = 709.5 Hz). HRMS (ESI-TOF) $C_{30}H_{31}FePSe$ [M]$^+$ *m/z*: calcd.: 558.0675, found: 558.0627.

*4.6.3. Synthesis of (Se)P(C≡CFc)(^{c}C$_4$H$_3$O)$_2$ (**4d**)*

100 mg (0.27 mmol) of **3d** were reacted with 25 mg (0.32 mmol) of elemental selenium. After appropriate work-up, **4d** was obtained as an orange solid. Yield: 122 mg (0.27 mmol, 100% based on **3d**). Anal. Calcd. for $C_{20}H_{15}FeO_2PSe$ (453.11 g/mol): C, 53.01; H, 3.34. Found: C, 53.40; H, 3.37. Mp.: 162 °C. IR (NaCl, ν/cm^{-1}): 575 (m, P–Se), 1005 (m, C–O), 1456 (w, P–C), 1549 (w, C=C), 2156 (vs, C≡C), 3108 (w, =C–H). ^{1}H NMR (500.30 MHz, $CDCl_3$, δ): 4.26 (s, 5 H, C$_5H_5$), 4.34 (pt, $^3J_{HH}$ = 1.9 Hz, C$_5H_4$), 4.60 (pt, $^3J_{HH}$ = 1.9 Hz, C$_5H_4$), 6.51 (dpt, $^4J_{HP}$ = 1.8 Hz, $^3J_{HH}$ = 3.5 Hz, $^3J_{HH}$ = 1.7 Hz, 2 H, H^4/C$_4H_3$O), 7.31 (m, 2 H, H^3/C$_4H_3$O), 7.74 (m, 2 H, H^5/C$_4H_3$O). ^{13}C{^{1}H} NMR (125.81 MHz, $CDCl_3$, δ): 60.1 (d, $^3J_{CP}$ = 5.1 Hz, C^i/C$_5$H$_4$), 70.6 (s, C$^\beta$/C$_5$H$_4$), 70.6 (s, C$_5$H$_5$), 72.8 (d, $^4J_{CP}$ = 1.5 Hz, C$^\alpha$/C$_5$H$_4$), 74.0 (d, $^1J_{CP}$ = 169.3 Hz, –C≡C–P), 108.6 (d, ^{2}JCP = 32.7 Hz, –C≡C–P), 111.6 (d, $^3J_{CP}$ = 10.2 Hz, C^4/C$_4$H$_3$O), 122.8 (d, $^2J_{CP}$ = 25.3 Hz, C^3/C$_4$H$_3$O), 145.4 (d, $^1J_{CP}$ = 132.1 Hz, C^2/C$_4$H$_3$O), 149.0 (d, $^4J_{CP}$ = 8.1 Hz, C^5/C$_4$H$_3$O). ^{31}P{^{1}H} NMR (202.53 MHz, $CDCl_3$, δ): –37.9 ($^1J_{PSe}$ = 783.9 Hz). HRMS (ESI-TOF) $C_{20}H_{15}FeO_2PSe$ [M]$^+$ *m/z*: calcd.: 453.9320, found: 453.9275.

*4.6.4. Synthesis of (Se)P(C≡CFc)(^{t}Bu)$_2$ (**4e**)*

100 mg (0.28 mmol) of **3e** were reacted with 27 mg (0.34 mmol) of selenium in its elemental form. After appropriate work-up, **4e** was obtained as an orange solid. Yield: 113 mg (0.28 mmol, 100% based on **3e**). Anal. Calcd. for $C_{20}H_{27}FePSe$ (433.21 g/mol): C, 55.45; H, 6.28. Found: C, 55.50; H, 6.19. Mp.: 165 °C. IR (NaCl, ν/cm^{-1}): 533 (m, P–Se), 1470 (m, P–C), 2158 (s, C≡C), 2868/2922/2962 (s, C–H), 3092 (w, =C–H). ^{1}H NMR (500.30 MHz, $CDCl_3$, δ): 1.46 (d, $^3J_{HP}$ = 17.3 Hz, 18 H, C(CH_3)$_3$), 4.24 (s, 5 H, C$_5H_5$), 4.27 (pt, $^3J_{HH}$ = 1.8 Hz, 2 H, C$_5H_4$), 4.52 (pt, $^3J_{HH}$ = 1.8 Hz, 2 H, C$_5H_4$). ^{13}C{^{1}H} NMR (125.81 MHz, $CDCl_3$, δ): 27.7 (d, $^2J_{CP}$ = 2.8 Hz, C(CH_3)$_3$), 38.4 (d, $^1J_{CP}$ = 41.9 Hz, C(CH_3)$_3$), 61.5 (d, $^3J_{CP}$ = 3.8 Hz, C^i/C$_5$H$_4$), 69.9 (s, C$^\beta$/C$_5$H$_4$), 70.1 (s, C$_5$H$_5$), 72.2 (d, $^4J_{CP}$ = 1.3 Hz, C$^\alpha$/C$_5$H$_4$), 75.0 (d, $^1J_{CP}$ = 114.2 Hz, -C≡C-P), 106.7 (d, $^2J_{CP}$ = 15.8 Hz, –C≡C–P). ^{31}P{^{1}H} NMR (202.53 MHz, $CDCl_3$, δ): 56.3 ($^1J_{PSe}$ = 715.3 Hz). HRMS (ESI-TOF) $C_{20}H_{27}FePSe$ [M + nNa]$^+$ *m/z*: calcd.: 457.0259, found: 457.0256.

*4.6.5. Synthesis of (Se)P(C≡CFc)(^{c}C$_6$H$_{11}$)$_2$ (**4f**)*

100 mg (0.25 mmol) of **3f** were reacted with 24 mg (0.30 mmol) of selenium. After appropriate work-up, **4f** was obtained as an orange solid. Yield: 121 mg (0.25 mmol, 100% based on **3f**). Anal. Calcd. for $C_{24}H_{31}FePSe$ (485.28 g/mol): C, 59.40; H, 6.44. Found: C, 60.12; H, 6.60. Mp.: 135 °C. IR (NaCl, ν/cm^{-1}): 526/536 (m, P–Se), 1448 (m, P–C), 2158 (s, C≡C), 2852/2928 (s, C–H), 3095 (w, =C–H). ^{1}H NMR (500.30 MHz, $CDCl_3$, δ): 1.24–1.78 (m, 11 H, C$_6H_{11}$), 1.91–2.09 (m, 11 H, C$_6H_{11}$), 4.26 (s, 5 H, C$_5H_5$), 4.30 (pt, $^3J_{HH}$ = 1.9 Hz, 2 H, C$_5H_4$), 4.55 (pt, $^3J_{HH}$ = 1.9 Hz, 2 H, C$_5H_4$). ^{13}C{^{1}H} NMR (125.81 MHz, $CDCl_3$, δ): 25.9 (d, J_{CP} = 8.0 Hz, C$_6H_{11}$), 25.9 (d, J_{CP} = 6.5 Hz, C$_6H_{11}$), 26.2 (d, J_{CP} = 15.5 Hz, C$_6H_{11}$), 26.4 (d, J_{CP} = 13.8 Hz, C$_6H_{11}$), 27.1 (d, J_{CP} = 4.4 Hz, C$_6H_{11}$), 38.3 (d, $^1J_{CP}$ = 50.9 Hz, C^1/C$_6H_{11}$), 61.3 (d, $^3J_{CP}$ = 3.6 Hz, C^i/C$_5$H$_4$), 70.0 (s, C$^\beta$/C$_5$H$_4$), 70.3 (s, C$_5$H$_5$), 72.5 (m, C$^\alpha$/C$_5$H$_4$), 74.5 (d, $^1J_{CP}$ = 118.4 Hz, –C≡C–P), 106.6 (d, $^2J_{CP}$ = 17.6 Hz, –C≡C–P). ^{31}P{^{1}H} NMR (202.53 MHz, $CDCl_3$, δ): 31.0 ($^1J_{PSe}$ = 712.5 Hz). HRMS (ESI-TOF) $C_{24}H_{31}FePSe$ [M]$^+$ *m/z*: calcd.: 486.0675, found: 486.0679.

*4.7. General procedure for the synthesis of palladium complexes **6e**, **6f** and **7a–f***

Phosphines **3a–3f** were reacted with 0.5 equivalents of [$PdCl_2$(cod)] (**5**) or [$PdCl_2(SEt_2)_2$] (**8**) in 40 mL of dry dichloromethane. The appropriate reaction solution was stirred for 2 h at ambient temperature. Afterward, the solvent was removed in vacuum and the residue was washed 5–6 times with 5 mL portions of diethyl ether. After drying in vacuum the appropriate complexes were obtained as red or brown solids.

*4.7.1. Synthesis of [Pd(Cl)(μ-Cl)(P(C≡CFc)^{t}Bu$_2$)]$_2$ (**6e**)*

0.5 g (1.41 mmol) of **3f** were reacted with 0.20 g (0.70 mmol) of **5**. After appropriate work-up, **6e** was isolated as a brown solid. Yield: 700 mg (0.66 mmol, 94% based on **5**). Anal. Calcd. for $C_{40}H_{54}Cl_4Fe_2P_2Pd_2$ (1063.15 g/mol): C, 45.19; H, 5.12. Found: C, 44.91; H, 5.16. Mp.: 156 °C. IR (KBr, ν/cm^{-1}): 1468 (w, P–C), 2155 (vs, C≡C), 2867/2890/2922/2966 (w, C–H), 3097 (w, =C–H). ^{1}H NMR (500.30 MHz, $CDCl_3$, δ): 1.62 (d, $^3J_{HP}$ = 16.9 Hz, 36 H, C(CH_3)$_3$), 4.28 (pt, $^3J_{HH}$ = 1.9 Hz, 4 H, C$_5H_4$), 4.32 (s, 10 H, C$_5H_5$), 4.58 (pt, $^3J_{HH}$ = 1.9 Hz, 4 H, C$_5H_4$). ^{13}C{^{1}H} NMR (125.81 MHz, $CDCl_3$, δ): 30.2 (d, $^2J_{CP}$ = 3.4 Hz, C(CH_3)$_3$), 40.2 (d, $^1J_{CP}$ = 24.5 Hz, C(CH_3)$_3$), 62.0 (m, C^i/C$_5$H$_4$), 70.0 (s, C$_5$H$_4$), 70.7 (s, C$_5$H$_5$), 72.7 (s, C$_5$H$_4$), 77.3 (C≡C–P*), 116.8 (s, –C≡C–P). ^{31}P{^{1}H} NMR (202.53 MHz, $CDCl_3$, δ): 49.7. HRMS (ESI-TOF) $C_{40}H_{54}Cl_4Fe_2P_2Pd_2$ [M – Cl]$^+$ *m/z*: calcd.: 1026.9536, found: 1026.9515* signal concealed by $CDCl_3$.

*4.7.2. Synthesis of [Pd(Cl)(μ-Cl)(P(C≡CFc)(^{c}C$_6$H$_{11}$)$_2$)]$_2$ (**6f**)*

0.5 g (1.23 mmol) of **3g** were reacted with 0.17 g (0.61 mmol) of **5**. After appropriate work-up, **6f** was obtained as a brown solid. Yield: 642 mg (0.55 mmol, 90% based on **5**). Anal. Calcd. for $C_{48}H_{62}Cl_4Fe_2P_2Pd_2$ (1167.30 g/mol): C, 52.58; H, 5.70. Found: C, 52.71; H, 5.65. Mp.: 200 °C (dec). IR (KBr, ν/cm^{-1}): 1446 (w, P–C), 1653 (w, C=C), 2151 (s, C≡C), 2851/2928 (vs, C–H), 3098 (w, =C–H). ^{1}H NMR (500.30 MHz, $CDCl_3$, δ): 1.26–1.37 (m, 8 H, C$_6H_{11}$), 1.75–2.01 (m, 20 H, C$_6H_{11}$), 2.21–2.38 (m, 8 H, C$_6H_{11}$), 2.52–2.58 (m, 4 H, C$_6H_{11}$), 2.88–2.92 (m, 4 H, C$_6H_{11}$), 4.28 (m, 4 H, C$_5H_4$), 4.29 (s, 10 H, C$_5H_5$), 4.56 (pt, $^3J_{HH}$ = 1.7 Hz, 4 H, C$_5H_4$). ^{13}C{^{1}H} NMR (125.81 MHz, $CDCl_3$, δ): 25.9 (, C^6/C$_6$H$_{11}$), 26.6 (m, C^2/^{3}/C$_6$H$_{11}$), 26.8 (m, C^2/^{3}/C$_6$H$_{11}$), 29.0 (m, C^4/^{5}/C$_6$H$_{11}$), 31.2 (s, C^4/^{5}/C$_6$H$_{11}$), 36.4 (d, $^1J_{CP}$ = 35.5 Hz, C^1/C$_6$H$_{11}$), 62.6 (s, C^i/C$_5$H$_4$), 70.2 (s, C$_5$H$_4$), 70.8 (s, C$_5$H$_5$), 72.8 (s, C$_5$H$_4$), 75.7 (d, $^1J_{CP}$ = 91.5 Hz, C≡C–P), 110.2 (pt, $^{2,3}J_{CP}$ = 5.3 Hz, C≡C–P). ^{31}P{^{1}H} NMR (202.53 MHz, $CDCl_3$, δ): 31.0. HRMS (ESI-TOF) $C_{48}H_{62}Cl_4Fe_2P_2Pd_2$ [M]$^+$ *m/z*: calcd.: 1167.9843, found: 1167.9851.

*4.7.3. Synthesis of [$PdCl_2$(P(C≡CFc)(2-MeC_6H_4)$_2$)$_2$] (**7b**)*

0.5 g (1.18 mmol) of **3b** were reacted with 0.17 g (0.59 mmol) of **5**. After appropriate work-up, **7b** was obtained as a red solid. Yield: 560 mg (0.55 mmol, 95% based on **5**). Anal. Calcd. for $C_{52}H_{46}Cl_2Fe_2P_2Pd \cdot 1/3\ CH_2Cl_2$ (1050.20 g/mol): C, 59.85; H, 4.48. Found: C, 60.14; H, 4.44. Mp.: 214 °C. IR (KBr, ν/cm^{-1}): 756 (s, =

C–H, *o*-disubst. benzene), 1448 (w, P–C), 1627 (C=C), 2159 (vs, C≡C), 2922/2963 (w, C–H), 3056/3081 (w, =C–H). ^{1}H NMR (500.30 MHz, $CDCl_3$, δ): 2.86 (s, 12 H, 2-CH_3C$_6$H$_4$), 4.24 (pt, $^3J_{HH}$ = 1.9 Hz, 4 H, C$_5H_4$), 4.25 (s, 10 H, C$_5H_5$), 4.55 (pt, $^3J_{HH}$ = 1.9 Hz, 4 H, C$_5H_4$), 5.30 (s, CH_2Cl$_2$), 7.18–7.41 (m, 12 H, H^{m,p}/2-CH$_3$C$_6H_4$), 7.77–7.86 (m, 4 H, Ho/2-CH$_3$C$_6H_4$). ^{13}C{^{1}H} NMR (125.81 MHz, $CDCl_3$, δ): 23.5 (pt, $^3J_{CP}$ = 4.0 Hz, 2-CH_3C$_6$H$_4$), 53.52 (s, CH_2Cl$_2$), 62.9 (m, C^i/C$_5$H$_4$), 69.7 (s, C$^\beta$/C$_5$H$_4$), 70.4 (s, C$_5$H$_5$), 72.3 (s, C$^\alpha$/C$_5$H$_4$), 74.9 (pt, $^1J_{CP}$ = 51.9 Hz, –C≡C–P), 111.4 (d, $^2J_{CP}$ = 9.2 Hz, –C≡C–P), 125.9 (pt, J_{CP} = 6.0 Hz, 2-CH$_3$C$_6$H$_4$), 126.8 (pt, $^1J_{CP}$ = 28.7. Hz, C^i/2-CH$_3$C$_6$H$_4$), 131.3 (s, C^p/2-CH$_3$C$_6$H$_4$), 131.5 (pt, J_{CP} = 4.2 Hz, 2-CH$_3$C$_6$H$_4$), 135.1 (pt, J_{CP} = 8.0 Hz, 2-CH$_3$C$_6$H$_4$), 142.6 (pt, J_{CP} = 5.5 Hz, 2-CH$_3$C$_6$H$_4$). ^{31}P{^{1}H} NMR (202.53 MHz, $CDCl_3$, δ): –6.8. HRMS (ESI-TOF) $C_{52}H_{46}Cl_2Fe_2P_2Pd$ [M]$^+$ *m*/*z*: calcd.: 1022.0186, found: 1022.0145; [M – Cl]$^+$ *m*/*z*: calcd.: 985.0511, found: 985.0487; [M]$^{2+}$ *m*/*z*: calcd.: 511.0090, found: 511.0083; [M – Cl]$^{2+}$ *m*/*z*: calcd.: 492.5253, found: 492.5236.

*4.7.4. Synthesis of [PdCl$_2$(P(C≡CFc)(2,4,6-Me$_3$C$_6$H$_4$)$_2$)$_2$] (**7c**)*

0.5 g (1.05 mmol) of **3c** were reacted with 0.15 g (0.52 mmol) of **5**. After appropriate work-up, **7c** could be isolated as a brown solid. Yield: 556 mg (0.49 mmol, 94% based on **5**). Anal. Calcd. for $C_{60}H_{62}Cl_2Fe_2P_2Pd$ (1134.10 g/mol): C, 63.54; H, 5.51. Found: C, 63.67; H, 5.69. Mp.: 172 °C. IR (KBr, ν/cm^{-1}): 818 (m, =C–H, *para*-subst. benzene), 1459 (m, P–C), 1603 (m, C=C), 2152 (s, C≡C), 2923/2963 (w, C–H), 3072 (w, =C–H). ^{1}H NMR (500.30 MHz, $CDCl_3$, δ): 2.24 (s, 6 H, 2,4,6-(CH_3)$_3$C$_6$H$_2$), 2.70 (s, 12 H, 2,4,6-(CH_3)$_3$C$_6$H$_2$), 4.19 (s, 5 H, C$_5H_5$), 4.20 (pt, $^3J_{HH}$ = 1.8 Hz, 2 H, C$_5H_4$), 4.49 (pt, $^3J_{HH}$ = 1.8 Hz, 2 H, C$_5H_4$), 6.84 (m, 4 H, 2,4,6-(CH$_3$)$_3$C$_6H_2$). ^{13}C{^{1}H} NMR (125.81 MHz, $CDCl_3$, δ): 21.1 (s, 2,4,6-(CH_3)$_3$C$_6$H$_2$), 25.6 (pt, $^3J_{CP}$ = 4.1 Hz, 2,4,6-(CH_3)$_3$C$_6$H$_2$), 64.2 (pt, $^3J_{CP}$ = 1.2 Hz, C^i/C$_5$H$_4$), 69.3 (s, C$^\beta$/C$_5$H$_4$), 70.1 (s, C$_5$H$_5$), 72.0 (s, C$^\alpha$/C$_5$H$_4$), 77.4 (pt, $^1J_{CP}$ = 66.7 Hz, C≡C–P), 109.1 (pt, $^2J_{CP}$ = 8.9 Hz, C≡C–P), 126.0 (pt, $^1J_{CP}$ = 27.6 Hz, C^i/2,4,6-(CH$_3$)$_3$C$_6$H$_2$), 130.7 (pt, $^3J_{CP}$ = 4.5 Hz, C^m/2,4,6-(CH$_3$)$_3$C$_6$H$_2$), 140.1 (s, C^p/2,4,6-(CH$_3$)$_3$C$_6$H$_2$), 142.5 (pt, $^2J_{CP}$ = 5.8 Hz, Co/2,4,6-(CH$_3$)$_3$C$_6$H$_2$). ^{31}P{^{1}H} NMR (202.53 MHz, $CDCl_3$, δ): –24.0. HRMS (ESI-TOF) $C_{60}H_{62}Cl_2Fe_2P_2Pd$ [M]$^+$ *m*/*z*: calcd.: 1134.1441, found: 1134.1351; [M – Cl]$^+$ *m*/*z*: calcd.: 1097.1765, found: 1097.1688; [M-nH-2Cl]$^+$ *m*/*z*: calcd.: 1061.2001, found: 1061.1929; [M-(C$_{30}$H$_{31}$FeP)PdCl$_2$]$^+$ *m*/*z*: calcd.: 478.1508, found: 478.1480.

*4.7.5. Synthesis of [PdCl$_2$(P(C≡CFc)(^{c}C$_4$H$_3$O)$_2$)$_2$] (**7d**)*

0.5 g (1.34 mmol) of **3d** were reacted with 0.19 g (0.67 mmol) of **5**. After appropriate work-up, **7d** was obtained as a dark red solid. Yield: 596 mg (0.64 mmol, 96% based on **5**). Anal. Calcd. for $C_{40}H_{30}Cl_2Fe_2O_4P_2Pd\cdots 1/4\ CH_2Cl_2$ (946.86 g/mol): C, 51.06; H, 3.25. Found: C, 51.05; H, 3.32. Mp.: >250 °C. IR (KBr, ν/cm^{-1}): 1010 (m, C–O), 1454 (w, P–C), 1573 (w, C=C), 2155 (s, C≡C), 3107 (w, =C–H). ^{1}H NMR (500.30 MHz, $CDCl_3$, δ): 4.12 (s, 5 H, C$_5H_5$), 4.26 (pt, $^3J_{HH}$ = 1.6 Hz, 2 H, C$_5H_4$), 4.32 (pt, $^3J_{HH}$ = 1.6 Hz, 2 H, C$_5H_4$), 5.30 (s, CH_2Cl$_2$), 6.53 (m, 2 H, H^4/C$_4H_3$O), 7.33 (m, 2 H, H^3/C$_4H_3$O), 7.70 (m, 2 H, H^2/C$_4H_3$O). ^{13}C{^{1}H} NMR (125.81 MHz, $CDCl_3$, δ): 53.52 (s, CH_2Cl$_2$), m60.8 (m, C^i/C$_5$H$_4$), 70.4 (s, C$_5$H$_4$), 70.6 (s, C$_5$H$_5$), 72.6 (s, C$_5$H$_4$), 73.7 (d, $^1J_{CP}$ = 60.0 Hz, C≡C–P), 94.6 (pt, $^2J_{CP}$ = 8.1 Hz, C≡C–P), 111.9 (pt, $^3J_{CP}$ = 4.4 Hz, C^4/C$_4$H$_3$O), 125.2 (d, $^2J_{CP}$ = 24.8 Hz, C^3/C$_4$H$_3$O), 148.8 (d, $^1J_{CP}$ = 99.1 Hz, C^2/C$_4$H$_3$O), 148.8 (pt, $^4J_{CP}$ = 3.3 Hz, C^5/C$_4$H$_3$O). ^{31}P{^{1}H} NMR (202.53 MHz, $CDCl_3$, δ): –32.4. HRMS (ESI-TOF) $C_{40}H_{30}Cl_2Fe_2O_4P_2Pd$ [M]$^+$ *m*/*z*: calcd.: 925.8727, found: 925.8656.

*4.7.6. Synthesis of [PdCl$_2$(P(C≡CFc)^{t}Bu$_2$)$_2$] (**7e**)*

0.5 g (1.41 mmol) of **3e** were reacted with 0.25 g (0.70 mmol) of **8**. After appropriate work-up, **7e** was obtained as an orange solid. Yield: 584 mg (0.66 mmol, 94% based on **8**). Anal. Calcd. for $C_{40}H_{54}Cl_2Fe_2P_2Pd$ (885.82 g/mol): C, 54.24; H, 6.14. Found: C, 53.75; H, 6.17. Mp.: 250 °C. IR (KBr, ν/cm^{-1}): 1459 (w, P–C), 1655 (w, C=C), 2162 (s, C≡C), 2863/2917/2955 (m, C–H), 3097 (w, =C–H). ^{1}H NMR (500.30 MHz, CD_2Cl_2, δ): 1.59 (t, $^3J_{HP}$ = 7.7 Hz Hz, 36 H, C(CH_3)$_3$), 4.25 (pt, $^3J_{HH}$ = 1.8 Hz, 4 H, C$_5H_4$), 4.28 (s, 10 H, C$_5H_5$), 4.54 (pt, $^3J_{HH}$ = 1.8 Hz, 4 H, C$_5H_4$). ^{13}C{^{1}H} NMR (125.81 MHz, $CDCl_3$, δ): 30.2 (pt, $^2J_{CP}$ = 3.4 Hz, C(CH_3)$_3$), 40.1 (pt, $^1J_{CP}$ = 24.5 Hz, C(CH$_3$)$_3$), 62.0 (m, C^i/C$_5$H$_4$), 70.0 (s, C$_5$H$_4$), 70.7 (s, C$_5$H$_5$), 72.7 (s, C$_5$H$_4$), 77.4 (C≡C–P*), 116.8 (m, C≡C–P). ^{31}P{^{1}H} NMR (202.53 MHz, $CDCl_3$, δ): 49.7. HRMS (ESI-TOF) $C_{40}H_{54}Cl_2Fe_2P_2Pd$ [M]$^+$ *m*/*z*: calcd.: 886.0808, found: 886.0780; [M – Cl]$^+$ *m*/*z*: calcd.: 849.1134, found: 849.1083; [M+nH-2Cl]$^+$ *m*/*z*: calcd.: 815.1526, found: 815.1471; [M]$^{2+}$ *m*/*z*: calcd.: 443.0401, found: 443.0332* signal concealed by $CDCl_3$.

*4.7.7. Synthesis of [PdCl$_2$(P(C≡CFc)(^{c}C$_6$H$_{11}$)$_2$)$_2$] (**7f**)*

0.5 g (1.23 mmol) of **3f** were reacted with 0.22 g (0.61 mmol) of **8**. After appropriate work-up, **7f** was obtained as an orange solid. Yield: 481 mg (0.58 mmol, 95% based on **8**). Anal. Calcd. for $C_{48}H_{62}Cl_2Fe_2P_2Pd$ (829.71 g/mol): C, 58.24; H, 6.31. Found: C, 58.34; H, 6.80. Mp.: 210 °C. IR (KBr, ν/cm^{-1}): 1447 (w, P–C), 1655 (w, C=C), 2158 (s, C≡C), 2849/2925 (s, C–H), 3075 (w, =C–H). ^{1}H NMR (500.30 MHz, CD_2Cl_2, δ): 1.28 (m, 4 H, H^6/C$_6H_{11}$), 1.39 (m, 8 H, H^2/^{3}/C$_6H_{11}$), 1.63 (m, 8 H, H^4/^{5}/C$_6H_{11}$), 1.74 (m, 4 H, H^6/C$_6H_{11}$), 1.86 (m, 8 H, H^2/^{3}/C$_6H_{11}$), 2.13 (m, 4 H, H^4/^{5}/C$_6H_{11}$), 2.45 (m, 4 H, H^4/^{5}/C$_6H_{11}$), 2.76 (m, 4 H, H^1/C$_6H_{11}$), 4.21 (s, 10 H, C$_5H_5$), 4.26 (pt, $^3J_{HH}$ = 1.5 Hz, 4 H, C$_5H_4$), 4.36 (pt, $^3J_{HH}$ = 1.5 Hz, 4 H, C$_5H_4$). ^{13}C{^{1}H} NMR (125.81 MHz, $CDCl_3$, δ): 25.2 (s, C^6/C$_6$H$_{11}$), 25.8 (pt, $^2J_{CP}$ = 5.7 Hz, C^2/^{3}/C$_6$H$_{11}$), 26.0 (pt, $^2J_{CP}$ = 8.0 Hz, C^2/^{3}/C$_6$H$_{11}$), 28.7 (m, C^4/^{5}/C$_6$H$_{11}$), 29.3 (s, C^4/^{5}/C$_6$H$_{11}$), 37.5 (dpt, $^1J_{CP}$ = 32.3 Hz, C^1/C$_6$H$_{11}$), 61.4 (m, C^i/C$_5$H$_4$), 68.9 (s, C$_5$H$_4$), 69.0 (s, C$_5$H$_5$), 71.0 (s, C$_5$H$_4$), 74.4 (d, $^1J_{CP}$ = 92.7 Hz, C≡C–P), 109.4 (pt, $^2J_{CP}$ = 5.1 Hz, C≡C–P). ^{31}P{^{1}H} NMR (202.53 MHz, $CDCl_3$, δ): 28.4. HRMS (ESI-TOF) $C_{48}H_{62}Cl_2Fe_2P_2Pd$ [M]$^+$ *m*/*z*: calcd.: 990.1437, found: 990.1377; [M – Cl]$^+$ *m*/*z*: calcd.: 953.1762, found: 953.1705; [M]$^{2+}$ *m*/*z*: calcd.: 495.0716, found: 495.0667; [M – Cl]$^{2+}$ *m*/*z*: calcd.: 477.5872, found: 477.5838.

4.8. Synthesis of [PdCl$_2$(P(C≡CFc)(^{c}C$_6$H$_{11}$)$_2$)$_2$][B(C$_6$F$_5$)$_4$]$_2$ ([7f][(B(C$_6$F$_5$)$_4$)]$_2$)

80 mg (0.096 mmol) of **7f** were dissolved in 20 mL of dry tetrahydrofuran, cooled to –60 °C and 83 mg (0.096 mmol) of [AgB(C$_6$F$_5$)$_4$]·Et$_2$O dissolved in 20 mL of dry tetrahydrofuran were added dropwise. The resulting yellow solution was slowly warmed to ambient temperature and stirred overnight. After concentration in vacuum to 5 mL, 20 mL of ^{n}hexane were added forming a dark precipitate. The supernatant layer was decanted and the precipitate was washed 3 times with 10 mL portions of ^{n}hexane. The product was obtained as a dark purple solid after drying it in vacuum. Yield: 95 mg (0.040 mmol, 42% based on **7f**). Anal. Calcd. for $C_{96}H_{62}B_2Cl_2F_{40}Fe_2P_2Pd$ (2348.04 g/mol): C, 49.11; H, 2.66. Found: C, 50.66; H, 3.89. Mp: 196 °C (dec.). IR (KBr, ν/cm^{-1}): 1465 (s, P–C), 1642 (w, C=C), 2146 (s, C≡C), 2856/2934 (s, C–H). HRMS (ESI-TOF) $C_{96}H_{62}B_2Cl_2F_{40}Fe_2P_2Pd$ [M- 2 B(C$_6$F$_5$)$_4$]$^{2+}$ *m*/*z*: calcd.: 953.1762, found: 953.1568.

4.9. General procedure for the Suzuki reaction

2-Bromo toluene (500 mg, 2.92 mmol) or 4′-chloro acetophenone (464 mg, 3.00 mmol), phenyl boronic acid (470 mg, 3.85 mmol), potassium carbonate (1.21 g, 8.76 mmol) and acetyl ferrocene (114 mg, 0.50 mmol) were dissolved in a dioxane-water mixture (12 mL, ratio 2:1, *v*/*v*). After addition of 0.1 mol% (reaction of 2-bromo toluene) or 0.5 mol% (reaction of 4′-chloro acetophenone) of the appropriate catalyst (**6e**, **6f**, **7a**–**f**), the reaction mixture was stirred for 1 h at 100 °C. Samples of 1 mL were taken

Table 5
Crystal and intensity collection data for **6e**, **6f**, **7b**, and **7c**.

	6e	**6f**	**7b**	**7c**
Formula weight	1063.07	1405.95	1260.56	1134.04
Chemical formula	$C_{40}H_{54}Cl_4Fe_2P_2Pd_2$	$C_{50}H_{64}Cl_{10}Fe_2P_2Pd_2$	$C_{54}H_{48}Cl_8Fe_2P_2Pd$	$C_{60}H_{62}Cl_2Fe_2P_2Pd$
Crystal system	Triclinic	Triclinic	Monoclinic	Triclinic
Space group	P −1	P-1	C2/c	P-1
a (Å)	7.8922(3)	11.1687(5)	16.5847(4)	10.7065(3)
b (Å)	11.3363(6)	12.0851(5)	15.3081(18)	11.1859(3)
c (Å)	12.7408(6)	12.3642(5)	21.4121(14)	11.7479(3)
α (°)	107.024(4)	108.658	90.02	70.779(2)
β (°)	92.317(3)	104.146	95.826(7)	78.395(2)
γ (°)	101.085(3)	110.544	90.0010(10)	74.904(2)
V (Å^3)	1063.92(9)	1355.68(10)	5408.0(7)	1272.35(6)
ρ_{calc} (g cm^{-3})	1.659	1.722	1.548	1.480
F(000)	536	708	2544	584
Crystal dimensions (mm)	0.2 × 0.2 × 0.1	0.1 × 0.1 × 0.05	0.05 × 0.05 × 0.05	0.2 × 0.1 × 0.08
Z	1	1	4	1
Max. and min. transmission	1.00000, 0.92315	1.00000, 0.30942	1.00000, 0.74777	1.00000, 0.95654
Absorption coefficient (λ, mm^{-1})	1.854	14.834	1.349	1.120
Scan range (°)	2.92–26.06	4.37–61.99	2.97–26.07	2.88–26.00
Index ranges	$-9 \le h \le 9$, $-14 \le k \le 14$, $-15 \le l \le 15$	$-12 \le h \le 12$, $-11 \le k \le 13$, $-14 \le l \le 14$	$-20 \le h \le 20$, $-18 \le k \le 18$, $-26 \le l \le 26$	$-13 \le h \le 13$, $-11 \le k \le 13$, $-14 \le l \le 13$
Total reflections	9450	10,537	15,697	12,216
Unique reflections	4174	4247	5113	4963
R_{int}	0.0205	0.0199	0.0844	0.0242
Data/restraints/para-meters	4174/0/226	4247/0/298	5113/0/303	4963/0/304
Goodness-of-fit on F^2	0.971	1.073	0.951	1.117
R_1[a], wR_2[a] [I 2ρ(I)]	0.0212, 0.0451	0.0233, 0.0636	0.0439, 0.0843	0.0315, 0.0877
R_1[a], wR_2[a] (all data)	0.0306, 0.0467	0.0262, 0.0653	0.0955, 0.1024	0.0432, 0.0939
Largest differences in peak and hole peak in final Fourier map (e Å^{-3})	0.550, −0.431	0.542, −0.575	0.766, −0.692	0.708, −0.670

[a] $R_1 = [\Sigma(||F_o| - |F_c||)/\Sigma|F_o|]$; $wR_2 = [\Sigma(w(F_o^2 - F_c^2)^2)/\Sigma(wF_o^4)]^{1/2}$; $S = [\Sigma w(F_o^2 - F_c^2)^2]/(n-p)^{1/2}$. n = number of reflections, p = parameters used.

after 2.5, 5, 10, 20, 30, and 60 min and chromatographed on silica gel with diethyl ether as eluent. All volatiles were evaporated under reduced pressure and the conversions were determined by ^{1}H NMR spectroscopy.

4.10. General procedure for the Heck reaction

Iodo benzene (612 mg, 3.0 mmol), *t*-butylacrylate (397 mg, 3.1 mmol), EtN^iPr_2 (452 mg, 3.5 mmol) and acetyl ferrocene (114 mg, 0.5 mmol) were dissolved in a toluene–acetonitrile mixture (15 mL, 1:1, *v*/*v*) and loaded with 0.5 mol% of the respective catalyst (**6e**, **6f**, **7a**–**7f**). The reaction mixture was stirred at 80 °C and samples (1 mL) were taken in periods of 1 h. The samples were chomatographed on silica gel with diethyl ether as eluent. All volatiles were evaporated and the conversions were determined by ^{1}H NMR spectroscopy.

4.11. Crystal structure determination

The crystal and intensity collection data for **6e**, **6f**, **7b**, and **7c** are summarized in Table 5. All data were collected on an Oxford Gemini S diffractometer with graphite monochromatized Mo K_α radiation ($\lambda = 0.71073$ Å) at 100 K (**6e**, **7b**, **7c**) and graphite monochromatized Cu K_α radiation ($\lambda = 1.54$ Å) at 110 K (**6f**). The structures were solved by direct methods using *SHELXS-97* [35] (**6e**, **6f**) or SIR-92 [36] (**7b**, **7c**) and refined by full-matrix least-square procedures on F^2 using *SHELXL-97* [37]. All *non*-hydrogen atoms were refined anisotropically and a riding model was employed in the refinement of the hydrogen atom positions.

Acknowledgment

We are grateful to the Deutsche Forschungsgemeinschaft and the Fonds der Chemischen Industrie for financial support.

Appendix A. Supplementary material

CCDC 838741; 838740; 838738; 838739 contain the supplementary crystallographic data for the compounds **6e**, **6f**, **7b** and **7c** respectively. These data can be obtained free of charge from The Cambridge Crystallographic Data Centre via www.ccdc.cam.ac.uk/data_request/cif.

Appendix. Supplementary material

Supplementary material associated with this article can be found, in the online version, at doi:10.1016/j.jorganchem.2012.01.017.

References

[1] For example: P.J. Low, T.M. Hayes, K.A. Udachin, A.E. Goeta, J.A.K. Howard, G.D. Enright, A.J. Carty J. Chem. Soc. Dalton Trans. (2002) 1455–1464 (and references cited therein).
[2] For example: (a) J. Fornies, E. Lalinde, A. Martin, M.T. Moreno, A.J. Welch, J. Chem. Soc. Dalton Trans. 1 (1995) 1333–1340;
(b) M. Bardaji, A. Laguna, Organometallics 20 (2001) 3906–3912;
(c) T. Baumgartner, K. Huynth, S. Schleidt, A.J. Lough, I. Manners, Chem. Eur. J. 8 (2002) 4622–4632;
(d) T. De Simone, R.S. Dickson, B.W. Skelton, A.W. White, Inorg. Chim. Acta 240 (1995) 323–333;
(e) I. Moldes, J. Ros, Inorg. Chim. Acta 232 (1995) 75–81.
[3] For example: (a) H. Lang, L. Zsolnai, Chem. Ber. (1991) 259–264;
(b) J. Fornies, M.A. Gomez-Saso, E. Lalinde, F. Martinez, M.T. Moreno, Organometallics 11 (1992) 2873–2883;
(c) J.R. Berenguer, L.R. Falvello, J. Fornies, E. Lalinde, M. Tomas, Organometallics 12 (1993) 6–7;
(d) J. Diez, M.P. Gamasa, J. Gimeno, E. Lastra, A. Villar, Eur. J. Inorg. Chem. 1 (2006) 78–87;
(e) F. Hong, Y. Ho, Y. Chang, Y. Lai, Tetrahedron 60 (2004) 2639–2645;
(f) H. Lang, M. Leise, A. Schmitzer, J. Organomet. Chem. 489 (1995) 77–81.
[4] For example: (a) E. Louattini, I. Moldes, J. Suades, J.F.M. Piniella, A. Alvarez-Larena, Organometallics 17 (1998) 3394–3397;
(b) J.P.H. Charmant, J. Fornies, J. Gomez, E. Lalinde, M.T. Moreno, A.G. Orpen, S. Solano, Angew. Chem. Int. Ed. 38 (1999) 3058–3061;

(c) Y. Miquel, A. Igau, B. Donnadieu, J.P. Mayoral, N. Pirio, P. Meunier, J. Am. Chem. Soc. 120 (1998) 3504–3505.
[5] For example: (a) B. Li, S. Xu, H. Song, B. Wang, Eur. J. Inorg. Chem. (2008) 5494–5504;
(b) C. Ledesma, A. Alvarez-Larena, J. Suades, J. Organomet. Chem. 693 (2008) 2775–2783;
(c) A. Diez, E. Lalinde, M.T. Moreno, S. Sanchez, Dalton Trans. (2009) 3434–3446.
[6] (a) B. Di Credico, F. Fabrizi de Biani, L. Gonsalvi, A. Guerri, A. Ienco, F. Laschi, M. Peruzzini, G. Reginato, A. Rossin, P. Zanello, Chem. Eur. J. 15 (2009) 11985–11998;
(b) T. Baumgartner, M. Fiege, F. Pontzen, R. Arteaga-Müller, Organometallics 25 (2006) 5657–5664 (and references cited therein).
[7] A. Jakob, B. Milde, P. Ecorchard, C. Schreiner, H. Lang, J. Organomet. Chem. 693 (2008) 3821–3830.
[8] A. Jakob, P. Ecorchard, M. Linseis, R.F. Winter, H. Lang, J. Organomet. Chem. 694 (2009) 655–666.
[9] For example: (a) D. Astruc, Anal. Bioanal. Chem. 399 (2011) 1811–1814;
(b) X.-F. Wu, P. Anbarasan, H. Neumann, M. Beller, Angew. Chem. Int. Ed. 49 (2010) 9047–9050;
(c) R. Jana, T.P. Pathak, M.S. Sigman, Chem. Rev. 111 (2011) 1417–1492;
(d) D. Steinborn, Grundlagen der metallorganischen Komplexkatalyse, Teubner, Wiesbaden, 2007;
(e) M. Beller, C. Bolm, Transition Metals for Organic Synthesis 2nd Edition, Wiley-VCH, Weinheim, 2004;
(f) B. Cornils, W.A. Herrmann, Applied Homogeneous Catalysis with Organometallic Compounds, VCH, Weinheim, 1996;
(g) F. Diederich, P.J. Stang, Metal-Catalyzed Cross Coupling Reactions 2nd Edition, Wiley-VCH, Weinheim, 2004.
[10] (a) S.-Y. Liu, M. J Choi, G.C. Fu, Chem. Comm. (2001) 2408–2409;
(b) T.E. Pickett, C.J. Richards, Tetrahedron 42 (2001) 3767–3769;
(c) D. Schaarschmidt, H. Lang, Cat. Commun. 11 (2010) 581–583;
(d) D. Schaarschmidt, H. Lang, Eur. J. Inorg. Chem. 30 (2010) 4811–4821;
(e) A.L. Boyes, I.R. Butler, S.C. Quayle, Tetrahedron Lett. 39 (1998) 7763–7766;
(f) O.V. Gusev, T.A. Peganova, A.M. Kalsin, N.V. Vologdin, P.V. Petrovskii, K.A. Layssenko, A.V. Tsvetkov, I.P. Beletskaya, Organometallics 25 (2006) 2750–2760;
(g) J.-C. Hierso, M. Beauperin, P. Meunier, Eur. J. Inorg. Chem. (2007) 3767–3780;
(h) T.J. Colacot, H.A. Shea, Org. Lett. 6 (2004) 3731–3734.
[11] For example: (a) A.T. Normand, K.J. Cavell, Eur. J. Inorg. Chem. (2008) 2781–2800;
(b) J.A. Loch, M. Albrecht, E. Peris, J. Mata, J.W. Faller, R.H. Crabtree, Organometallics 21 (2002) 700–706;
(c) X. Xu, B. Xu, Y. Li, S.H. Hong, Organometallics 29 (2010) 6343–6349;
(d) N. Debono, A. Labande, E. Manoury, J.-C. Daran, R. Poli, Organometallics 29 (2010) 1879–1882;
(e) J.-Y. Lee, P.-Y. Cheng, Y.-H. Tsai, G.-R. Lin, S.-P. Liu, M.-H. Sie, H.M. Lee, Organometallics 29 (2010) 3901–3911;
(f) C. Zhang, M.L. Trudell, Tetrahedron Lett. 41 (2000) 595–598.
[12] For example: (a) C. Baillie, L. Zhang, J. Xiao, J. Org. Chem. 69 (2004) 7779–7782;
(b) S. Nadri, M. Joshaghani, E. Rafiee, Organometallics 28 (2009) 6281–6287;
(c) W.A. Herrmann, M. Elison, J. Fischer, C. Köcher, G.R.J. Artus, Angew. Chem. Int. Ed. Engl. 34 (1995) 2371–2374;
(d) J.P. Wolfe, S.L. Buchwald, Angew. Chem. Int. Ed. Engl. 38 (1999) 2413–2416.
[13] For example: (a) W.A. Herrmann, V.P.W. Böhm, J. Organomet. Chem. 572 (1999) 141–145;
(b) A. Zapf, M. Beller, Chem. Eur. J. 7 (2001) 2908–2915.
[14] (a) S. Vuoti, M. Haukka, J. Pursiainen, J. Organomet. Chem. 692 (2007) 5044–5052;
(b) P. Zoufala, R. Gyepes, P. Stepnicka, J. Organomet. Chem. 689 (2004) 3556–3566;
(c) S. Vuoti, J. Autio, M. Laitila, M. Haukka, J. Pursiainen, Eur. J. Inorg. Chem. (2008) 397–407;
(d) S.J. Coles, P. Faulds, M.B. Hursthouse, D.G. Kelly, G.C. Ranger, A.J. Toner, N.M. Walker, J. Organomet. Chem. 586 (1999) 234–240;
(e) J.O. Yu, E. Lam, J.L. Sereda, N.C. Rampersad, A.J. Lough, C.S. Browning, D.H. Farrar, Organometallics 24 (2005) 37–47.(f) J.J. Stone, R.A. Stockland Jr., N.P. Rath, Inorg. Chim. Acta 342 (2003) 236–240;
(g) R.A. Baber, A.G. Orpen, P.G. Pringle, M.J. Wilkinson, R.L. Wingad, Dalton Trans. (2005) 659–667.
[15] (a) R.P. Pinnell, C.A. Megerle, S.L. Manatt, P.A. Kroon, J. Am. Chem. Soc. 95 (1973) 977–978;
(b) D.W. Allen, B.F. Taylor, J. Chem. Soc. Dalton Trans. 37 (1982) 51–54;
(c) D.W. Allen, I.W. Nowell, J. Chem. Soc. Dalton Trans. (1985) 2505–2508;
(d) A. Suarez, M.A. Mendez-Rojas, A. Pizzano, Organometallics 21 (2002) 4611–4621;
(e) D.J.M. Snelders, C. van der Burg, M. Lutz, A.L. Spek, G. van Koten, R.J.M. Klein Gebbink, Chem. Cat. Chem. 2 (2010) 1425–1437;
(f) S. Jeulin, S. Duprat de Paule, V. Ratovelomanana-Vidal, J.-P. Genet, N. Champion, P. Dellis, Angew. Chem. Int. Ed. 43 (2004) 320–325;
(g) B. Milde, M. Lohan, C. Schreiner, T. Rüffer, H. Lang, Eur. J. Inorg. Chem. (2011) 5437–5449.
[16] (a) C.A. Tolman, Chem. Rev. 77 (1977) 313–348;
(b) C.A. Tolman, W.C. Seidel, L.W. Gosser, J. Am. Chem. Soc. 96 (1974) 53–60.
[17] (a) J.M. Smith, B.C. Taverner, N.J. Coville, J. Organomet. Chem. 530 (1997) 131–140;
(b) B.C. Taverner, STERIC, Program for Calculation of Cone Angles, University of the Witwatersrand/South Africa, 1996.
[18] F. Barriere, R.U. Kirss, W.E. Geiger, Organometallics 24 (2005) 48–52.
[19] G. Gritzner, J. Kuta, Pure Appl. Chem. 56 (1984) 461–466.
[20] (a) J.C. Kotz, C.L. Nivert, J. Organomet. Chem. 52 (1973) 387–406;
(b) J.C. Kotz, C.L. Nivert, J.M. Lieber, J. Organomet. Chem. 91 (1975) 87–95;
(c) J. Podlaha, P. Stepnicka, J. Ludvik, I. Cisarova, Organometallics 15 (1996) 543–550;
(d) M.A. Bennett, S.K. Bhargava, A.M. Bond, I.M. Burgar, S.-X. Guo, G. Kar, S.H. Priver, J. Wagler, A.C. Willis, A.A.J. Torriero, Dalton Trans. 39 (2010) 9079–9090.
[21] (a) B.D. Swartz, C. Nataro, Organometallics 24 (2005) 2447–2451;
(b) C. Amatore, M. Azzabi, A. Jutand, J. Am. Chem. Soc. 113 (1991) 8375–8384;
(c) C. Amatore, M. Azzabi, A. Jutand, J. Am. Chem. Soc. 113 (1991) 1670–1677.
[22] (a) F. Paul, C. Lapinte, Coord. Chem. Rev. 178-180 (1998) 431–509;
(b) D.M. D'Alessandro, F.R. Keene, Chem. Soc. Rev. 35 (2006) 424–440;
(c) W. Kaim, B. Sarkar, Coord. Chem. Rev. 251 (2007) 584–594.
[23] (a) M. Lohan, P. Ecorchard, T. Rüffer, F. Justaud, C. Lapinte, H. Lang, Organometallics 28 (2009) 1878–1890;
(b) A. Hildebrandt, D. Schaarschmidt, H. Lang, Organometallics 30 (2011) 556–563.
[24] (a) N.S. Hush, Electrochim. Acta 13 (1968) 1005–1023;
(b) C. Lapinte, J. Organomet. Chem. 693 (2008) 793–801;
(c) D. Astruc, Electron Transfer and Radical Processes in Transition-Metal Chemistry, VCH, New York, 1995.
[25] B.S. Brunschwig, C. Creutz, N. Sutin, Chem. Soc. Rev. 31 (2002) 168–184.
[26] (a) M. Sato, Y. Hayashi, Organometallics 15 (1996) 721–728;
(b) M.I. Bruce, P.J. Low, F. Hartl, P.A. Humphrey, F. de Montigny, M. Jevric, C. Lapinte, G.J. Perkins, R.L. Roberts, B.W. Skelton, A.H. White, Organometallics 24 (2005) 5241–5255.
[27] For example: (a) S. Dietrich, A. Nicolai, H. Lang, J. Organomet. Chem. 696 (2011) 739–747;
(b) I.P. Beletskaya, A.V. Cheprakov, Chem. Rev. 100 (2000) 3009–3066.
[28] For example: (a) W.A. Herrmann, C. Brossmer, C.-P. Reisinger, T.H. Riermeier, K. Öfele, M. Beller, Chem. Eur. J. 3 (1997) 1357–1364;
(b) A.F. Littke, G.C. Fu, J. Org. Chem. 64 (1999) 10–11;
(c) J.P. Wolfe, R.A. Singer, B.H. Yang, S.L. Buchwald, J. Am. Chem. Soc. 121 (1999) 9550–9561;
(d) H. Weissman, D. Milstein, Chem. Commun. (1999) 1901–1902;
(e) N. Kataoka, Q. Shelby, J.P. Stambuli, J.F. Hartwig, J. Org. Chem. 67 (2002) 5553–5566.
[29] M.B. Robin, P. Day, Adv. Inorg. Chem. Radiochem 10 (1967) 247–360.
[30] J. Polin, H. Schottenberger, Org. Synth. 73 (1996) 262–267.
[31] (a) P.W. Clark, B.W. Mulraney, J. Organomet. Chem. 217 (1981) 51–59;
(b) P.W. Dyer, J. Fawcett, M.J. Hanton, Organometallics 27 (2008) 5082–5087;
(c) N.G. Andersen, R. McDonald, B.A. Keaya, Tetrahedron: Asymmetry 12 (2001) 263–269;
(d) H. Tomori, J.M. Fox, S.L. Buchwald, J. Org. Chem. 65 (2000) 5334–5341.
[32] D. Drew, J.R. Doyle, Inorg. Synth. 28 (1990) 348–349.
[33] D. Zim, A.L. Monteiro, J. Dupont, Tetrahedron Lett. 41 (2000) 8199–8202.
[34] (a) M. Krejcik, M. Danek, F. Hartl, J. Electroanal. Chem. 317 (1991) 179–187;
(b) A. Hildebrandt, T. Rüffer, E. Erasmus, J.C. Swarts, H. Lang, Organometallics 29 (2010) 4900–4905.
[35] G.M. Sheldrick, Acta Cryst., Sect. A 46 (1990) 467–473.
[36] A. Altomare, G. Cascarano, C. Giacovazzo, A. Gualardi, J. Appl. Cryst 26 (1993) 343–350.
[37] G.M. Sheldrick, SHELXL-97, Program for Crystal Structure Refinement, University of Göttingen, 1997.